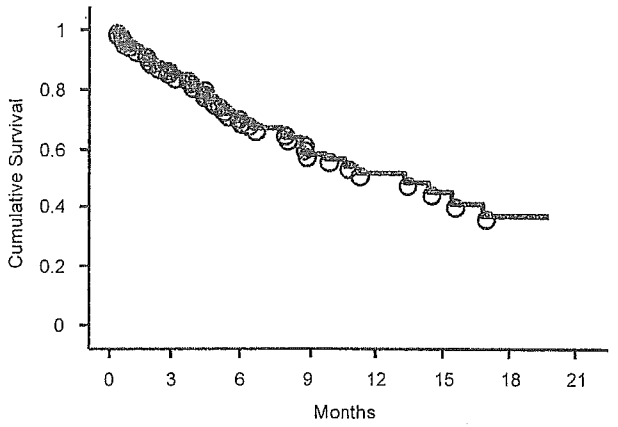

Figure 1. *Kaplan-Meier method of overall survival in all 122 patients. Median survival time was 14.4 months.*

patients with non-adenocarcinomas ($p<0.01$) (Figure 2C). The survival of patients with PS 0 to 2 was prolonged significantly longer compared to that of patients with PS 3 to 4 ($p<0.01$) (data not shown).

A multivariate analysis was carried out using the Cox hazard proportional model with significant prognostic factors identified in the univariate analyses (Table IV). Never smoked ($p<0.05$) and good PS (PS 0 to 2) ($p<0.01$) remained independent significant prognostic factors statistically, and female patients tended to have better survival in the multivariate analysis ($p=0.07$).

Toxicity. Most treated patients were assessable for toxicity (Table V). The main toxicity was Grade 1 or 2 rash, seen in 52.5% patients. Grade 1 or 2 pruritis and diarrhea were seen in 27.9% and 24.6%, respectively. Of the 122, 4.1% of patients and 2.5% of patients developed Grade 3 anorexia and rash, respectively. In addition, 8 patients (6.6%) stopped gefitinib due to diarrhea, nail change, nausea, anorexia, or elevated transaminases.

Four patients developed gefitinib-related interstitial pneumonitis. Two of them were complicated with interstitial pneumonitis, and one with radiation pneumonitis prior to gefitinib, although their pulmonary diseases were clinically stable. Three of the 4 were males. One patient recovered by stopping gefitinib and 2 patients recovered by stopping gefitinib and beginning steroid treatment. However, one patient died from progression of interstitial pneumonitis despite steroid treatment (Table VI).

Discussion

In the present analysis, we retrospectively analyzed the efficacy of 250mg/day gefitinib for patients with NSCLC.

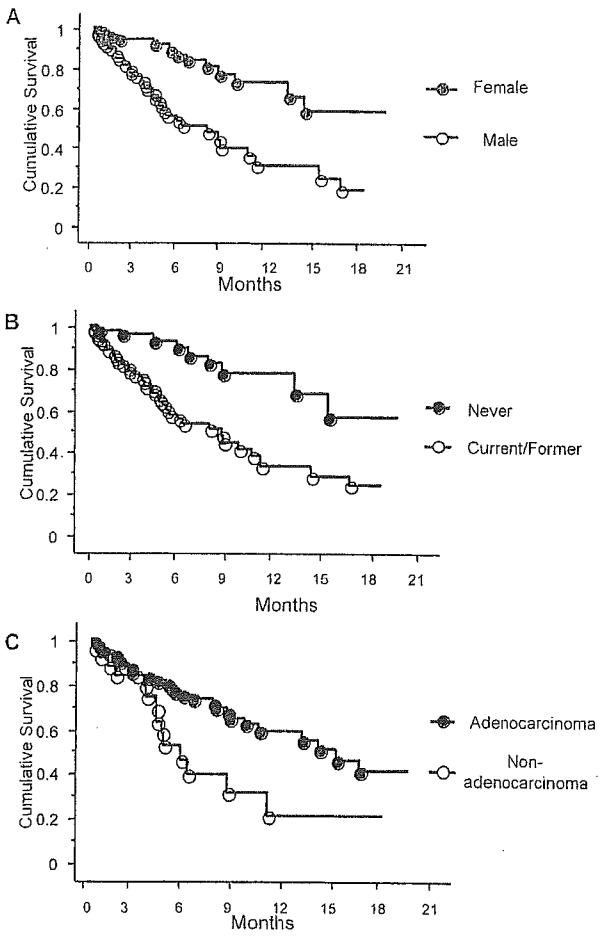

Figure 2. *Kaplan-Meier method of overall survival according to each patient's characteristics. (a) Overall survival is shown separately on the basis of gender. (b) Overall survival is shown separately on the basis of never having smoked and current/former smokers. (c) Overall survival is shown separately on the basis of patients with adenocarcinoma and non-adenocarcinoma. The survival differences in each category are statistically different ($p<0.01$).*

The objective response rate was 24.6% of the total patient population. Two phase II trials of gefitinib in patients with pretreated advanced NSCLC (IDEAL 1 and IDEAL 2) demonstrated antitumor activity (objective response rates, 11.8% to 18.4%) (15, 16), whereas the response rates were higher for Japanese patients (27.5%) than non-Japanese patients (10.4%) (15). The response rate in the present analysis was comparable to that of Japanese patients in IDEAL 1. The median survival was 14.4 months in the present analysis. In IDEAL 1 and IDEAL 2, the median survival was 7.6 months and 7 months, respectively. Subset analysis of data from the Japanese patients in IDEAL 1 showed that median survival was 414 days, which is comparable to the present data (21).

Table IV. *Multivariable analysisa of features associated with improved survival.*

Characteristics	Hazard Ratio	95% CI	*P*
Gender			
Male	0.46	0.20 to 1.08	0.07
Female	1		
Smoking habit			
Never	2.59	1.02 to 6.62	0.046
Current/Former	1		
Histology			
Non-adenocarcinoma	0.70	0.37 to 1.32	0.27
Adenocarcinoma	1		
Performance status			
3-4	0.18	0.08 to 0.37	<0.0001
0-2	1		

[a]Cox hazard analysis

Table V. *Treatment-related toxicity (%).*

	Grade 1/2	Grade 3	Grade 4
Rash	52.5	2.5	0
Pruritus	27.9	0.8	0
Diarrhea	24.6	0.8	0
Anorexia	13.1	4.1	0
Dry skin	14.8	0.8	0
Nail changes	8	0	0
Dehydration	2.5	1.6	0
GOT or GPT[a]	5.7	0.8	0
Intersitial pneumonitis	2.5	0	0.8

[a]Elevated liver transaminase

Table VI. *Characteristics of patients with interstitial pneumonitis.*

No.	Age	Gender	History	Smoking habit	PS	No. of former chemotherapy	Prior pulmonary complications	Length (day)	Adverse effect	Current status
1	74	M	SCC[a]	Yes	1	0	Interstitial pneumonitis	47	Rash Diarrhea	Death[c]
2	74	M	Ad[b]	No	1	2	Interstitial pneumonitis	24	No	Ceased
3	70	M	Ad[b]	Yes	1	2	Radiation pneumonitis	52	Rash Pruritus Nail changes Dry skin	Ceased
4	76	F	Ad[b]	No	1	1	No	71	Rash Pruritus Nail changes Dry skin Diarrhea	Ceased

[a]Squamous cell carcinoma
[b]Adenocarcinoma
[c]Possibly therapy-related death

We also analyzed the association between sensitivity to gefitinib and patient characteristics. In the present analysis, gender and smoking habit were associated with favorable tumor response, and four factors were associated with improved survival in patients receiving gefitinib; females, never smoked, adenocarcinoma and good PS in the univariate analysis. Among them, smoking habit was predictive of tumor response in the multivariate analysis, although no statistical difference was observed ($p=0.08$). In addition, good PS (PS 0 to 2) and never smoked remained independent prognostic factors and female patients tended to have better survival in the multivariate analysis. Previously, multivariate analysis of all patients in IDEAL 1 revealed that PS, gender, histology and prior immuno/hormonal therapy were significant prognostic factors associated with objective tumor response (15). Subset analysis of data from Japanese patients in IDEAL 1 showed that survival was longer in patients with adenocarcinoma, those with symptom improvement, or female patients in the univariate analysis, but not in the multivariate analysis (21). Moreover, Janne *et al.* reported that significant independent prognostic factors associated

with improved survival were females, good PS and adenocarcinoma (22). Our results are almost comparable to these results and confirmed the result of subset analysis of Japanese patients in IDEAL 1.

Miller *et al.* reported that bronchioloalveolar carcinoma was a more significant prognostic factor for gefitinib sensitivity than adenocarcinoma (23). We had only one patient with bronchioloalveolar carcinoma, who showed an objective response. In the present analysis, most of the patients were diagnosed by small specimens of transbronchial lung biopsy, by which it was difficult to definitely diagnose bronchioloalveolar carcinoma, and we were unable to analyze the association between tumor response and bronchioloalveolar carcinoma

The present analysis included 20 patients with no previous chemotherapy. Among them, 5 patients showed a tumor response (25%), which was almost compatible with that in patients with previous chemotherapy (24.5%) in the present analysis. In addition, the median survival of patients with no previous chemotherapy was 8.6 months. There are few reports about the efficacy of gefitinib monotherapy as first-line therapy. Argiris *et al.* reported that 25 patients, who were unfit or refused chemotherapy, received 250mg oral gefitinib daily as first-line therapy for the treatment of NSCLC, and 4 of the 22 evaluable patients (18%) had an objective response (24). The median time to progression was 2.2 months, median survival was 12.6 months and 1-year survival was 52% (24). The present results were compatible with this former analysis and suggested that gefitinib was effective as first-line therapy. Gefitinib monotherapy should undergo further evaluation as first-line therapy in advanced NSCLC.

In the present analysis, the median duration of treatment with gefitinib for patients with PR or SD was 7.6 months and many patients received gefitinib for a long time. There are few precise reports on long duration of treatment with gefitinib. The present results suggested that the efficacy of gefitinib could be sustainable for a long time and long duration of treatment could contribute to the prolongation of survival.

Recently, somatic mutations in the tyrosine kinase domain of the EGFR gene have been shown to be correlated with clinical responsiveness to gefitinib (25, 26). Screening for such mutations in lung cancers may identify patients who will have a response to gefitinib, as does being female, having adenocarcinoma and never having smoked. We have not yet analyzed whether the 30 patients with objective responses have specific mutations in the EGFR gene and investigation for EGFR mutations would definitely be needed in the future study.

Major adverse events were rash, pruritis, diarrhea and anorexia, which is consistent with previous reports. Patients given gefitinib have been documented to develop severe acute interstitial pneumonitis (17). In the present analysis, 4 patients developed interstitial pneumonitis, and one died of it. Three of them had a history of prior pulmonary complications. Although the cause of interstitial pneumonitis by gefitinib is unknown, the frequency of interstitial pneumonitis in Japanese patients tends to be higher than in non-Japanese patients, and may be related to population or environmental differences.

In conclusion, gefitinib showed favorable antitumor activity for patients with NSCLC, particularly females, never smokers, or patients with adenocarcinoma. On the other hand, one patient died from gefitinib-related interstitial pneumonitis and closer investigation is required in patients with prior pulmonary complications.

References

1 Ginsberg RJ, Vokes EE and Raben A: Non-small cell lung cancer. *In*: De Vita VT, Hellmann S, Rosenberg SA (eds): Cancer: Principles and Practice of Oncology. Ed. 6, Philadelphia, Lippincott-Raven Publishers 858-910, 2001.

2 Bunn PA: Treatment of advanced non-small-cell lung cancer with two-drug combinations. J Cin Oncol *20*: 3565-3567, 2002.

3 Non-Small Cell Lung Cancer Collaborative Group: Chemotherapy in non-small cell lung cancer–A meta-analysis using updated data on individual patients from 52 randomized clinical trials. BMJ *311*: 899-909, 1995.

4 Grilli R, Oxyman AD and Julian JA: Chemotherapy for advanced non-small-cell lung cancer: how much benefit is enough? J Clin Oncol *11*: 1866-1872, 1993.

5 Shepherd FA, Fossella FV, Lynch T, Arm JP, Rigas JR and Kris MG: Docetaxel (Taxotere) shows survival and quality-of-life benefits in the second-line treatment of non-small cell lung cancer: a view of two phase III trials. Semin Oncol *28*: 4-9, 2001.

6 Fossella FV, De Vore R, Kerr RN, Crawford J, Natale RR, Dunphy F *et al*: Randomized phase III trial of docetaxel *versus* vinorelbine or ifosfamide in patients with advanced non-small-cell lung cancer previously treated with platinum-containing chemotherapy regimens. The TAX 320 Non-Small Cell Lung Cancer Study Group. J Clin Oncol *18*: 2354-2362, 2000.

7 Pavelic K, Banjac Z, Pavelic J and Spavebti S: Evidence for a role of EGF receptor in the progression of human lung carcinoma. Anticancer Res *13*: 1133-1137, 1993.

8 Fujino S, Enokibori T, Tezuka N, Asada Y, Inoue S, Kato H *et al*: A comparison of epidermal growth factor receptor levels and other prognostic parameters in non-small cell lung cancer. Eur J Cancer *32A*: 2070-2074, 1996.

9 Baselga J: New technologies in epidermal growth factor receptor-targeted cancer therapy. Signal *1*: 12-21, 2000.

10 Wells A: The epidermal growth factor receptor (EGFR): a new target in cancer therapy. Signal *1*: 4-11, 2000.

11 Woodburn JR: The epidermal growth factor receptor and its inhibition in cancer therapy. Pharmacol Ther *82*: 241-250, 1999.

12 Lawrence DS and Niu J: Protein kinase inhibitors: the tyrosine-specific protein kinases. Pharmacol Ther *77*: 81-114, 1998.

13 Herbst RS, Maddox AM, Rothenberg ML, Small EJ, Rubin EH, Baselga J *et al*: Selective oral epidermal growth factor receptor tyrosine kinase inhibitor ZD1839 is generally well-tolerated and has activity in non-small-cell lung cancer and other solid tumors: results of a phase I trial. J Clin Oncol *20*: 3815-3825, 2002.
14 Baselga J, Rischin D, Ranson M, Calvert H, Raymond E, Kieback DG *et al*: Phase I safety, pharmacokinetic, and pharmacodynamic trial of ZD1839, a selective epidermal growth factor receptor tyrosine kinase inhibitor, in patients with five selected solid tumor types. J Clin Oncol *20*: 4292-4302, 2002.
15 Fukuoka M, Yano S, Giaccone G, Tamura T, Nakagawa K, Douillard JY *et al*: Multi-institutional randomized phase II trial of gefitinib for previously treated patients with advanced non-small-cell lung cancer. J Clin Oncol *21*: 2237-2246, 2003.
16 Kris MG, Natale RB, Herbst RS, Lynch TJ Jr, Prager D, Belani CP *et al*: Efficacy of gefitinib, an inhibitor of the epidermal growth factor receptor tyrosine kinase, in symptomatic patients with non-small cell lung cancer. JAMA *290*: 2149-2158, 2003.
17 Inoue A, Saijo Y, Maemondo M, Gomi K, Tokue Y, Kimura Y *et al*: Severe acute interstitial pneumonia and gefitinib. Lancet *361*: 137-139, 2003.
18 Histological Typing of Lung and Pleural Tumors, Ed 3. International Histological Classification of Tumours, World Health Orgnization. Geneva 1999.
19 American Joint Committee on Cancer: Lung. *In*: Beahrs OH, Henson DE, Hutter RVP, Kennedy BJ (eds). Manual for Staging of Cancer. Philadelphia Lippincott 115-122, 1992.
20 Therasse P, Arbuck SG, Eisenhauer EA, Wanders J, Kaplan RS, Rubinstein L *et al*: New guidelines to evaluate the response to treatment in solid tumors. J Natl Cancer Inst *92*: 205-216, 2000.
21 Nishiwaki Y, Yano S, Tamura T, Nakagawa K, Kudoh S, Horai T *et al*: Subset analysis of data in the Japanese patients with NSCLC from IDEAL 1 study on gefitinib. Jpn J Cancer Chemother *31*: 567-573, 2004.
22 Janne PA, Gurubhagavatula S, Yeap BY, Lucca J, Ostler P, Skarlin AT *et al*: Outcomes of patients with advanced non-small cell lung cancer treated with gefitinib (ZD1839, 'Iressa') on an expanded access study. Lung Cancer *44*: 221-230, 2004.
23 Miller VA, Kris MG, Shah N, Patel J, Azzoli C, Gomez J *et al*: Bronchioloalveolar pathologic subtype and smoking history predict sensitivity to gefitinib in advanced non-small-cell lung cancer. J Clin Oncol *22*: 1103-1109, 2004.
24 Argiris A and Mittal N: Gefitinib as first-line, compassionate use therapy in patients with advanced non-small-cell lung cancer. Lung Cancer *43*: 317-322, 2004.
25 Paez JG, Janne PA, Lee JC, Tracy S, Greulich H, Gabriel S *et al*: EGFR mutations in lung cancer: correlation with clinical response to gefitinib therapy. Science *304*: 1497-1500, 2004.
26 Lynch TJ, Bell DW, Sordella R, Gurubhagavatula S, Okimoto RA, Brannigan BW *et al*: Activating mutations in the epidermal growth factor receptor underlying responsiveness of non-small-cell lung cancer to gefitinib. N Engl J Med *350*: 129-39, 2004.

Received August 19, 2004
Accepted December 17, 2004

Laboratory/Clinical Translational Research

Oncology

Oncology 2005;69:301–310
DOI: 10.1159/000089680

Received: January 20, 2005
Accepted after revision: May 28, 2005
Published online: November 9, 2005

Expression of N-Acetylglucosaminyltransferase V in the Development of Human Esophageal Cancers: Immunohistochemical Data from Carcinomas and Nearby Noncancerous Lesions

Yoko Ishibashi[a] Hirotoshi Dosaka-Akita[a] Eiji Miyoshi[f] Masanobu Shindoh[d] Masaki Miyamoto[b] Ichiro Kinoshita[a] Hiroki Miyazaki[a] Tomoo Itoh[e] Satoshi Kondo[b] Masaharu Nishimura[c] Naoyuki Taniguchi[f]

[a]Department of Medical Oncology, [b]Department of Surgical Oncology and [c]First Department of Medicine, Hokkaido University Graduate School of Medicine, [d]Department of Oral Pathobiological Science, Hokkaido University Graduate School of Dental Medicine and [e]Department of Surgical Pathology, Hokkaido University Hospital, Sapporo, and [f]Department of Biochemistry, Osaka University Medical School/ Graduate School of Medicine, Suita, Japan

Key Words
GnT-V · Carcinogenesis · Esophageal cancer · L4-PHA · Ki-67

Abstract
Objective: N-Acetylglucosaminyltransferase V (GnT-V) is a key enzyme in the formation of branching asparagine-linked oligosaccharides and is linked to tumor invasion and metastasis in colon and breast cancers. In normal esophageal epithelium, β1,6-branched asparagine-linked oligosaccharides synthesized by GnT-V are seen in the basal cell layers but not in the superficial cell layers, and its presence has been shown in invasive esophageal cancers. However, neither GnT-V expression nor its clinical significance has been previously examined in human normal, premalignant and malignant esophageal tissues. ***Methods:*** GnT-V expression was studied by immunohistochemistry using a specific monoclonal antibody in 121 surgically resected specimens of esophageal squamous cell carcinomas (SCCs) and adjacent tissues, and was analyzed statistically in relation to various characteristics. ***Results:*** GnT-V expression was observed in none (0%) of the 19 normal epithelial tissues, 1 (2%) of the 43 hyperplastic tissues, 30 (54%) of the 56 mildly dysplastic tissues, 27 (63%) of the 43 moderately dysplastic tissues, 21 (44%) of the 48 in situ SCCs and 29 (26%) of the 110 invasive SCCs ($p < 0.005$). GnT-V expression was observed significantly more frequently in mildly and moderately dysplastic tissues when compared with normal epithelial and hyperplastic tissues ($p < 0.005$), and its frequency was decreased in in situ and invasive SCCs ($p < 0.005$). GnT-V expression was frequently observed in SCCs of small size and without distant metastasis or lymph node metastasis. ***Conclusions:*** Increased expression of GnT-V is associated with the early event of esophageal tumorigenesis.

KARGER
Fax +41 61 306 12 34
E-Mail karger@karger.ch
www.karger.com

0030–2414/05/0694–0301$22.00/0

Accessible online at:
www.karger.com/ocl

Hirotoshi Dosaka-Akita
Department of Medical Oncology, Hokkaido University Graduate School of Medicine
North 15, West 7, Kita-ku
Sapporo, 060-8638 (Japan)
Tel. +81 11 706 5021, Fax +81 11 706 5077, E-Mail hdakita@med.hokudai.ac.jp

Introduction

The prognosis for esophageal carcinoma remains poor, although advances in surgical techniques and chemoradiotherapy have improved survival to some extent. The overall 5-year survival rate generally remains at less than 50%, despite the use of multimodality therapy [1–5]. A better understanding of the molecular basis of esophageal carcinogenesis and identification of prognostically important biological markers are needed in order to improve survival.

It is known that sugar chains have a variety of functions and play key roles in development, differentiation, cell adhesion and cell growth [6, 7]. An enzyme that specifically catalyzes β1,6 branching of N-acetylglucosamine is UDP-N-acetylglucosamine:mannoside β1,6-N-acetylglucosaminyltransferase (GnT-V). This enzyme transfers N-acetylglucosamine from UDP-N-acetylglucosamine to α-*D*-6 mannoside of asparagine-linked oligosaccharides [8]. This enzyme has been shown to be linked to tumor metastasis [9–14]. High expression levels of the GnT-V gene are correlated with distant or lymph node metastasis and poor prognosis in human colorectal and breast cancer [15–17]. On the other hand, GnT-V expression is an early event in rat and human hepatocarcinogenesis [12, 18], and levels of GnT-V expression do not correlate with postsurgical prognosis in patients with hepatoma [18], thus suggesting that GnT-V is involved in or associated with the early stages of tumorigenesis. In normal esophageal epithelium, β1,6-branched asparagine-linked oligosaccharides synthesized by GnT-V are seen in basal cell layers but not in superficial cell layers [19], and its presence has been observed frequently in invasive esophageal cancers [20]. However, neither GnT-V expression nor its biological and clinical significance has been examined in human normal, premalignant or malignant esophageal tissues.

In the present study, we immunohistochemically studied GnT-V expression in 121 human esophageal squamous cell carcinomas (SCCs) and surrounding tissues in order to elucidate the significance of GnT-V in the development of esophageal cancers. We also investigated the presence of β1,6-branched asparagine-linked oligosaccharides transferred by GnT-V using *Phaseolus vulgaris* leukoagglutinin (L4-PHA) staining, which specifically binds to β1,6 branching [16], in order to examine the relationship between GnT-V expression and β1,6 branch synthesis.

Materials and Methods

Patients and Esophageal Specimens

One hundred and twenty-one patients (105 men and 16 women; mean age 62.3 years) with primary esophageal SCC underwent radical esophagectomy at the Department of Surgical Oncology, Hokkaido University Hospital, and its affiliated hospitals (Teinekeijinkai Hospital and Hokkaido Gastroenterology Hospital) between September 1989 and May 1999. In all cases, informed consent was obtained for the use of resected tumor specimens. No distant metastasis was detected in any patients on preoperative examination. No patients had received anticancer treatment before surgery. The clinical staging of tumors was determined according to the TNM classification system of the International Union Against Cancer [21].

Survival was analyzed for the 70 patients who met the following criteria: (1) they did not die in hospital after surgery; (2) they did not die of causes other than esophageal cancer within 3 years after surgery, and (3) patients who remained alive were followed up for more than 3 years after surgery. Fifty-one patients who did not meet the above criteria were excluded from survival analysis.

All specimens were fixed in 10% formalin and embedded in paraffin wax. One of the deepest sections from each tumor was selected for evaluation, and 4-μm serial sections were examined by immunohistochemistry. For lectin blotting, samples were immediately frozen in liquid nitrogen and stored at −80°C until use.

Immunohistochemistry for GnT-V and Ki-67

Expression of GnT-V and Ki-67 was analyzed by immunohistochemistry. Briefly, the labeled streptavidin biotin method was used with 4-μm serial sections of formalin-fixed, paraffin-embedded tissues after deparaffinization. For immunostaining of Ki-67, deparaffinized tissue sections were autoclaved in 10 m*M* citrate buffer (pH 6.0) for 10 min at 121°C in order to retrieve antigenicity. Sections were then immersed in methanol containing 1.5% hydrogen peroxide for 20 min in order to block endogenous peroxidase activity and were incubated with normal rabbit serum in order to block nonspecific antibody-binding sites. Sections were consecutively reacted with a mouse monoclonal antibody against recombinant human GnT-V [17] at a dilution of 1:1,600, with mouse monoclonal antibody MIB-1 (Immunotech, Marseilles, France) at a dilution of 1:50, or with control mouse isotype-specific immunoglobulin at 4°C overnight. Immunostaining was performed using the biotin-streptavidin immunoperoxidase method with 3,3′-diaminobenzidine as a chromogen (SAB-PO kit; Nichirei, Tokyo, Japan). Methyl green was used as the counterstain.

L4-PHA Histochemistry

L4-PHA lectin binds preferentially to GlcNAc residues on β1,6 branches of tri- and tetra-antennary sugar chains, which are products of GnT-V [22]. For staining with L4-PHA, deparaffinized tissue sections were incubated with 0.3% hydrogen peroxidase in methanol for 20 min at room temperature in order to eliminate endogenous peroxidase activity. Trypsinization [Tris buffer containing 0.1% trypsin (Difco Laboratories, Detroit, Mich., USA) and 0.1% $CaCl_2$, for 10 min at 37°C] was then performed. To remove sialylation of oligosaccharides, sections were treated with neuraminidase from *Vibrio cholerae* (Roche, Tokyo, Japan) at a concentration of 0.1 U/ml in sodium acetate buffer (pH 5.6) containing 0.04 *M* $CaCl_2$ for 1 h at 37°C. Sections were incubated with 5%

skim milk in PBS for 20 min at room temperature in order to block nonspecific staining and were then incubated with biotinylated L4-PHA lectins (EY Laboratories, San Mateo, Calif., USA) at a dilution of 1:500 at 4°C overnight. Staining was performed using the biotin-streptavidin immunoperoxidase method with 3,3'-diaminobenzidine as a chromogen (SAB-PO kit; Nichirei, Tokyo, Japan). Methyl green was used as the counterstain.

Evaluation of Staining

Expression of GnT-V in SCCs was classified as positive or negative, according to the proportion of positively stained cancer cells. Tumors having cytoplasmic staining in at least 10% of cancer cells were judged to be positive for GnT-V expression, while tumors having cytoplasmic staining in less than 10% of cancer cells were judged to be negative. Noncancerous lesions were considered positively stained when any cytoplasmic staining was present in the Golgi localization pattern.

L4-PHA staining was classified as high or low, according to the proportion of positively stained cells ($\geq$30% or <30%, respectively). For GnT-V and L4-PHA staining, sections were examined by two independent observers without prior knowledge of the clinical or clinicopathological status of the specimens.

Ki-67 labeling index (LI) was defined as the percentage of tumor cells displaying nuclear immunoreactivity and was calculated by counting the number of nuclear Ki-67-stained tumor cells among 1,000 tumor cells in each section. A single representative tissue section from each tumor was surveyed for Ki-67 microscopically at $\times$100 for at least two or three random areas. Cell counts were performed at $\times$400 in at least seven fields in these areas, using a Videomicrometer (Model VM-30; Olympus, Tokyo, Japan) equipped with a light microscope. Ki-67 LIs were reliably and reproducibly obtained using this Videomicrometer system.

Lectin Blot Analysis

Tissues were homogenized with a glass homogenizer in TNE buffer containing 10 m*M* Tris-HCl (pH 7.8), 1% NP-40, 0.15 *M* NaCl, 1 m*M* EDTA and a mixture of protease inhibitors (Wako, Osaka, Japan). Homogenized tissues were placed on ice for 20 min and were centrifuged at 15,000 rpm for 15 min at 4°C. The supernatant fraction was saved as the postnuclear supernatant and protein concentrations were determined with a BCA kit (Pierce, Rockford, Ill., USA) using bovine serum albumin as a standard. For lectin blot analysis, 20 μg of proteins were electrophoresed on a 10% polyacrylamide gel and then transferred onto a nitrocellulose membrane. After blocking with PBS containing 3% BSA overnight at 4°C, the membrane was incubated with 1 μg/ml of biotinylated L4-PHA (Seikagaku, Tokyo, Japan) for 3 h. Washing and developing were as described previously [23]. Reactive glycoprotein bands were visualized by chemiluminescence using an ECL system (Amersham Pharmacia Biotech UK, Little Chalfont, UK).

Statistical Analysis

Associations between GnT-V expression and categorical variables were analyzed by χ^2 test or Fisher's exact test, as appropriate. Associations between GnT-V expression and age or labeling indices were analyzed by Student's t test. Associations between Ki-67 LIs and categorical variables were analyzed by Student's t test. Differences in GnT-V expression among normal, premalignant and malignant tissues were analyzed by the Kruskal-Wallis test. Survival curves were estimated using the Kaplan-Meier method, and differences in survival distributions were evaluated by the generalized Wilcoxon test. Cox's proportional hazards modeling of factors potentially related to survival was performed in order to identify which factors might have a significant influence on survival. The significance level chosen was $p < 0.05$, and all tests were two-sided.

Results

Typical immunostaining patterns for GnT-V in normal, premalignant and malignant esophageal tissues are shown in figure 1. In tumor cells, GnT-V expression was seen in the Golgi localization pattern (fig. 1), as well as in noncancerous dysplastic epithelial cells. GnT-V expression was observed in none (0%) of the 19 normal epithelial tissues, 1 (2%) of the 43 hyperplastic tissues, 30 (54%) of the 56 mildly dysplastic tissues, 27 (63%) of the 43 moderately dysplastic tissues, 21 (44%) of the 48 in situ SCCs and 29 (26%) of the 110 invasive SCCs ($p < 0.005$ by the Kruskal-Wallis test) (fig. 2). GnT-V expression was observed significantly more frequently in mildly and moderately dysplastic tissues when compared with normal epithelial and hyperplastic tissues ($p < 0.005$), and when compared with in situ and invasive SCCs ($p < 0.005$). The relationship between GnT-V expression and various clinical and clinicopathological features of SCCs is summarized in table 1. In SCCs, tumors exhibiting GnT-V expression were smaller than tumors without GnT-V expression ($p = 0.03$). GnT-V expression was observed significantly more frequently in distant metastasis-negative tumors than in positive tumors ($p = 0.045$), and tended to be found more frequently in lymph node metastasis-negative tumors than in positive tumors ($p = 0.09$).

We next analyzed the relationship between GnT-V expression and patient survival (fig. 3) and the importance of GnT-V as a prognostic factor (table 2). GnT-V expression was not associated with survival (3-year survival rates, 36% for patients having tumors with negative GnT-V expression and 45% for patients having tumors with positive GnT-V expression; $p = 0.4$) (fig. 3), and was not a significant prognostic factor in univariate analysis (table 2). Univariate analysis for overall survival using a Cox proportional hazards model identified pT classification, pN classification, pM classification, pStage, surgical margin, and lymphatic invasion as significant prognostic predictors (table 2). Multivariate analysis of the same set of patients showed that pT classification, pN classification and surgical margin had independent prognostic values, with hazards ratios of 2.51 ($p = 0.01$), 2.83 ($p = 0.008$) and 3.25 ($p = 0.008$), respectively (table 2).

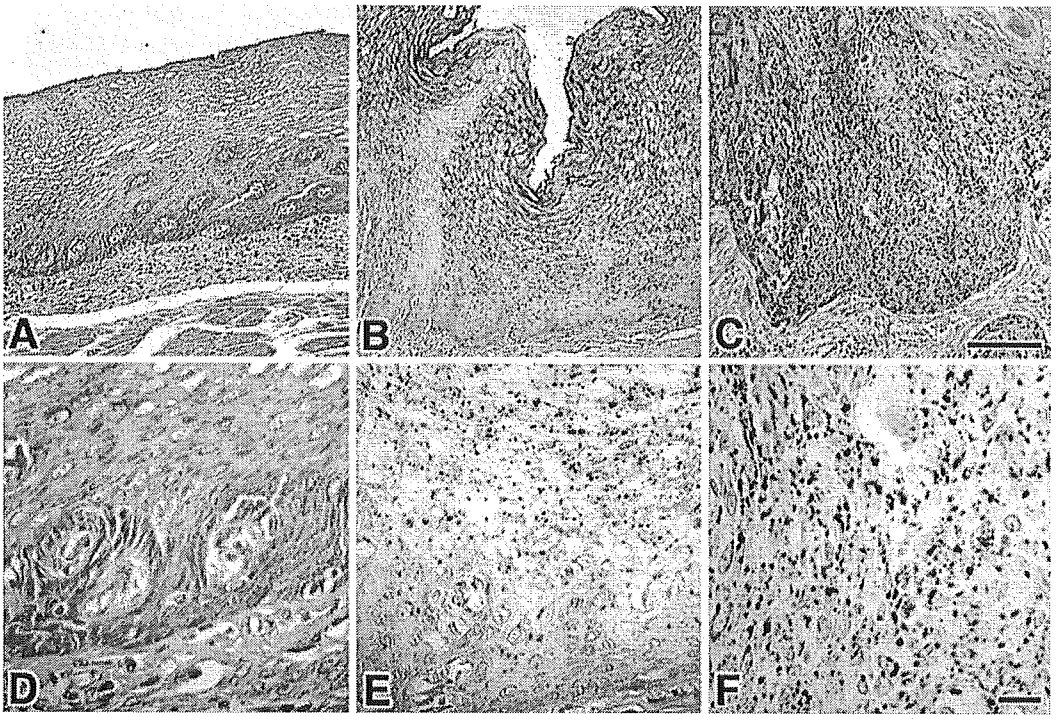

Fig. 1. Immunohistochemical staining patterns for GnT-V in normal epithelium, mild dysplasia and SCCs of the esophagus. GnT-V expression is not observed in normal epithelium (**A**, **D**), but is observed in mild dysplasia (**B**, **E**) and SCCs (**C**, **F**) in the Golgi localization pattern. Scale bar = 100 μm for **A–C** and 20 μm for **D–F**.

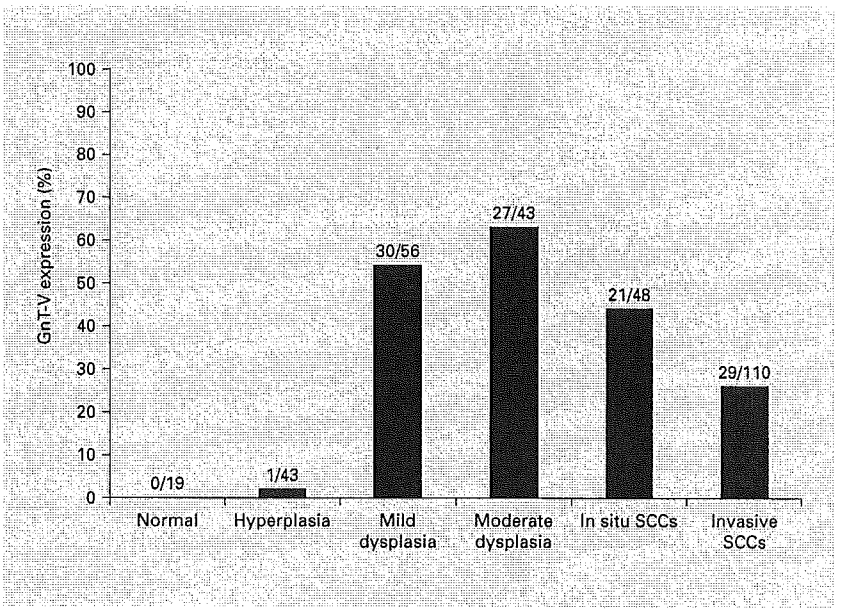

Fig. 2. GnT-V expression in esophageal SCCs and adjacent tissues. GnT-V expression was observed in none (0%) of the 19 normal epithelial tissues, 1 (2%) of the 43 hyperplastic tissues, 30 (54%) of the 56 mildly dysplastic tissues, 27 (63%) of the 43 moderately dysplastic tissues, 21 (44%) of the 48 in situ SCCs and 29 (26%) of the 110 invasive SCCs ($p < 0.005$ by the Kruskal-Wallis test).

Table 1. Relationship between GnT-V expression and clinical and clinicopathological characteristics in surgically resected esophageal SCCs

Characteristics	GnT-V expression		p
	positive (n = 38)	negative (n = 83)	
Age (mean ± SD), years	62.4 ± 8.9	62.3 ± 8.0	0.9
Sex			
Men	31	74	0.3
Women	7	9	
Tumor size (mean ± SD), cm	4.22 ± 2.19	5.31 ± 2.71	0.03
Tumor size[a]			
≥4.5 cm	15	48	0.09
<4.5 cm	23	35	
Grade			
G1	9	23	0.8
G2	19	42	
G3	10	18	
pT classification			
T1	19	35	0.5
T2–4	19	48	
pN classification			
N0	23	35	0.09
N1	15	48	
pM classification			
M0	35	63	0.045
M1	3	20	
pStage			
I	14	24	0.2
II	11	23	
III	10	16	
IV	3	20	
Lymphatic invasion			
+	21	46	1.0
–	17	37	
Vascular invasion			
+	13	28	1.0
–	25	55	
Double cancers			
Yes	10	14	0.3
No	28	69	
Ki-67 LI (mean ± SD)	46.7 ± 22.5 (n = 35)	44.9 ± 15.1 (n = 77)	0.6

[a] Tumors were divided into two groups based on the median value (4.5 cm) of tumor size.

Table 2. Cox's proportional hazards model analysis of potential prognostic factors

Characteristics	Hazards ratio (95% CI)	p
Univariate analysis		
Age (≥60/<60)	1.42 (0.77–2.64)	0.3
Sex (men/women)	2.43 (0.59–10.06)	0.2
Tumor size (≥4.5 cm/<4.5 cm)	1.69 (0.91–3.12)	0.09
Grade (2, 3/1)	1.21 (0.54–2.74)	0.6
pT classification (2, 3, 4/1)	3.42 (1.69–6.99)	0.0007
pN classification (1/0)	3.91 (1.94–7.81)	0.0001
pM classification (1/0)	2.53 (1.33–4.82)	0.005
pStage (II–IV/I)	3.90 (1.53–9.90)	0.004
Lymphatic invasion (+/–)	2.55 (1.33–4.88)	0.005
Vascular invasion (+/–)	1.86 (1.00–3.45)	0.051
Surgical margin (positive/negative)	4.69 (2.02–10.87)	0.0003
Double cancers (yes/no)	0.92 (0.44–1.91)	0.8
Adjuvant therapy (no/yes)	1.01 (0.59–1.93)	0.8
Performance status (1/0)	1.10 (0.46–2.59)	0.8
GnT-V expression (positive/negative)	0.80 (0.42–1.50)	0.5
Ki-67 LI (≥45%/<45%) (n = 63)	1.55 (0.83–2.89)	0.2
Multivariate analysis[a]		
Model 1		
pT classification (2, 3, 4/1)	2.51 (1.20–5.24)	0.01
pN classification (1/0)	2.83 (1.31–6.10)	0.008
pM classification (1/0)	1.30 (0.65–2.58)	0.5
Model 2		
pStage (II–IV/I)	2.82 (0.97–8.13)	0.06
Lymphatic invasion (+/–)	1.41 (0.65–3.02)	0.4
Surgical margin (positive/negative)	3.25 (1.37–7.72)	0.008

[a] Significant prognostic factors selected based on the results of univariate analysis.

The presence of β1,6-branched asparagine-linked oligosaccharides usually synthesized by GnT-V was then investigated using L4-PHA histochemistry in 14 randomly selected SCCs with positive GnT-V expression and 35 randomly selected SCCs with negative GnT-V expression (all specimens obtained from the Hokkaido University Hospital). In normal esophageal epithelium, expression of β1,6-branched asparagine-linked oligosaccharides is found in the basal cell layers but not in the superficial cell layers (fig. 4). On the other hand, high L4-PHA staining was observed in all of the 49 in situ and invasive SCCs (obviously more than 30% and at least 70% of tumor cells were stained) (fig. 4). In addition, hyperplastic and dysplastic tissues adjacent to SCCs were also positive for L4-PHA staining (data not shown).

In order to confirm the results of L4-PHA histochemistry, lectin blot analysis was performed. In lectin blotting using L4-PHA, which preferentially recognizes β1,6 branching, increases in β1,6 branching were observed in SCC tissues when compared with normal epithelial tissues in all five pairs of samples analyzed (fig. 5). These

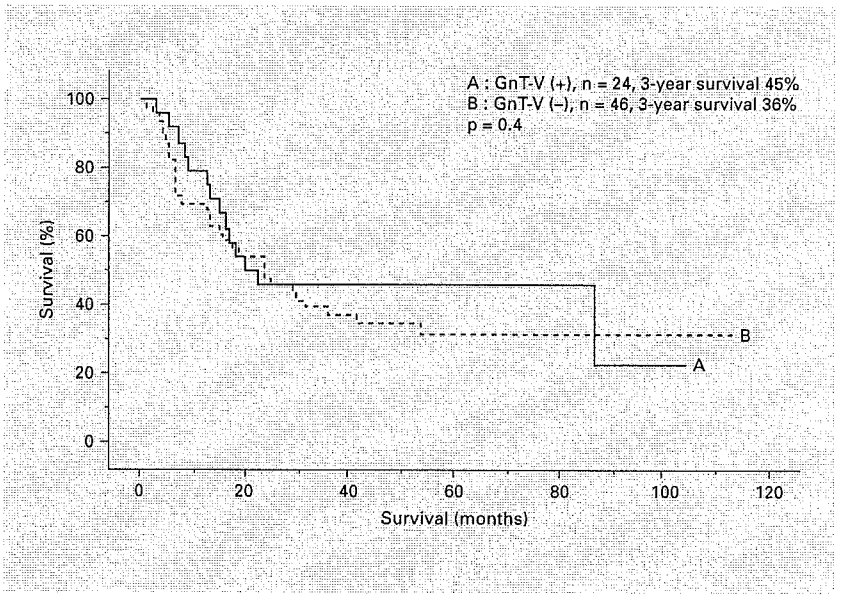

Fig. 3. Kaplan-Meier survival curves for patients with esophageal SCCs. Survival curves are stratified by positive (A) and negative (B) GnT-V expression.

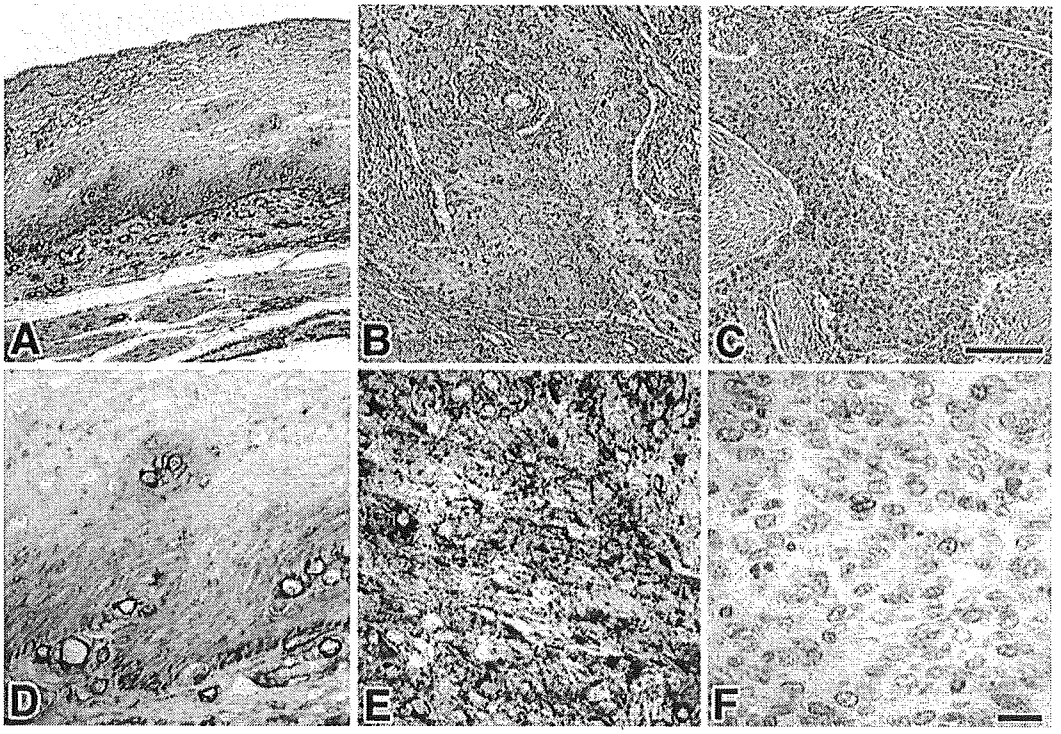

Fig. 4. Histochemical staining patterns for L4-PHA in normal epithelium and in esophageal SCCs. L4-PHA-reactive glycoconjugates are found in the basal cell layer but not in the superficial cell layer of normal epithelium (**A**, **D**). Positive L4-PHA staining (**B**, **E**) is observed diffusely in tumor cells in SCC without GnT-V expression (**C**, **F**). Scale bar = 100 μm for **A–C** and 20 μm for **D–F**.

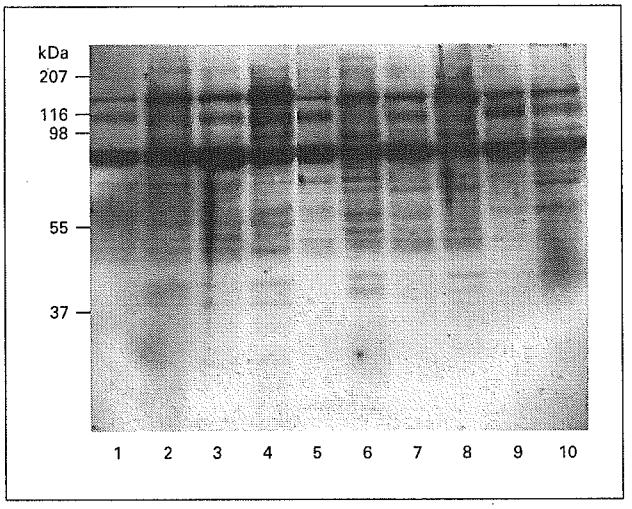

Fig. 5. Lectin blot analysis using L4-PHA on human esophageal SCC tissues. Proteins (20 μg) extracted from SCC tissues (lanes 2, 4, 6, 8 and 10) and surrounding normal esophageal epithelium (lanes 1, 3, 5, 7 and 9) were analyzed by Western blotting using L4-PHA. Increases in β1,6 branching were observed in SCC tissues when compared with normal epithelium. Lanes 1 and 2, 3 and 4, 5 and 6, 7 and 8, and 9 and 10 were prepared from the same patients.

results were consistent with results of L4-PHA histochemistry, which showed high L4-PHA staining in SCCs.

We then analyzed the relationship between GnT-V expression and tumor cell proliferation, as determined by Ki-67 LI. A monoclonal antibody MIB-1 recognizes a recombinant part of the Ki-67 nuclear antigen expressed during G1, S and G2/M phases, but not G0 phase, of the cell cycle [24]. Thus, the fraction of Ki-67-positive cells, Ki-67 LI, in tumor cells demonstrates tumor proliferative activity [25]. Ki-67 LI was determined in 113 of the 121 SCCs examined. The mean value of Ki-67 LIs was 46.0% (SD: 18.0%; range: 11.0–89.0%). To define an appropriate cutoff level for Ki-67 LIs in the subsequent analyses, we looked at their distribution among SCCs. Ki-67 LIs were considerably skewed and consisted of two populations with a cutoff level of 45%. Accordingly, tumors were divided into two groups having 'low' or 'high' Ki-67 LI: one group with a Ki-67 LI <45%, and the other group with a Ki-67 LI ≥45%. High Ki-67 LI was found in 58 (51%) of the 113 tumors, and low Ki-67 LI was found in 55 (49%). There was no relationship between Ki-67 LI and GnT-V expression. The relationship between Ki-67 LI and various clinical and clinicopathological features of SCCs is summarized in table 3. In SCCs, Ki-67 LI was significantly higher in T2–4 tumors than in T1 tumors ($p = 0.03$), in lymph node metastasis-positive tumors than in negative tumors ($p = 0.002$), and in vascular invasion-positive tumors than in negative tumors ($p = 0.005$). Ki-67 LI tended to be higher in lymphatic invasion-positive tumors than in negative tumors ($p = 0.08$), and in high-

Table 3. Relationship between Ki-67 LI and clinical and clinicopathological characteristics in surgically resected esophageal SCCs

Characteristics	Ki-67 LI (%, mean ± SD)	n	p
Age, years			
≥60	45.3 ± 17.7	71	0.6
<60	47.4 ± 18.5	42	
Sex			
Men	47.1 ± 17.9	98	0.1
Women	38.9 ± 16.9	15	
Tumor size[a]			
≥4.5 cm	48.2 ± 18.0	62	0.2
<4.5 cm	43.5 ± 17.8	51	
Grade			
G1	40.8 ± 18.6	31	0.06
G2, 3	48.0 ± 17.4	82	
pT classification			
T1	41.7 ± 17.5	48	
T2	45.1 ± 16.0	13	
T3	48.2 ± 16.7	40	
T4	57.6 ± 21.5	12	
T1	41.7 ± 17.5	48	0.03
T2–4	49.3 ± 17.7	65	
pN classification			
N0	40.4 ± 17.6	51	0.002
N1	50.7 ± 17.0	62	
pM classification			
M0	45.8 ± 18.4	89	0.8
M1	47.1 ± 16.6	24	
Lymphatic invasion			
+	48.6 ± 18.3	66	0.08
–	42.5 ± 17.1	47	
Vascular invasion			
+	52.6 ± 20.6	38	0.005
–	42.7 ± 15.6	75	
Double cancers			
Yes	38.9 ± 16.8	25	0.02
No	48.1 ± 17.8	88	
GnT-V expression in cancer			
Positive	47.1 ± 22.2	36	0.5
Negative	44.9 ± 15.1	77	

[a] Tumors were divided into two groups based on the median value (4.5 cm) of tumor size.

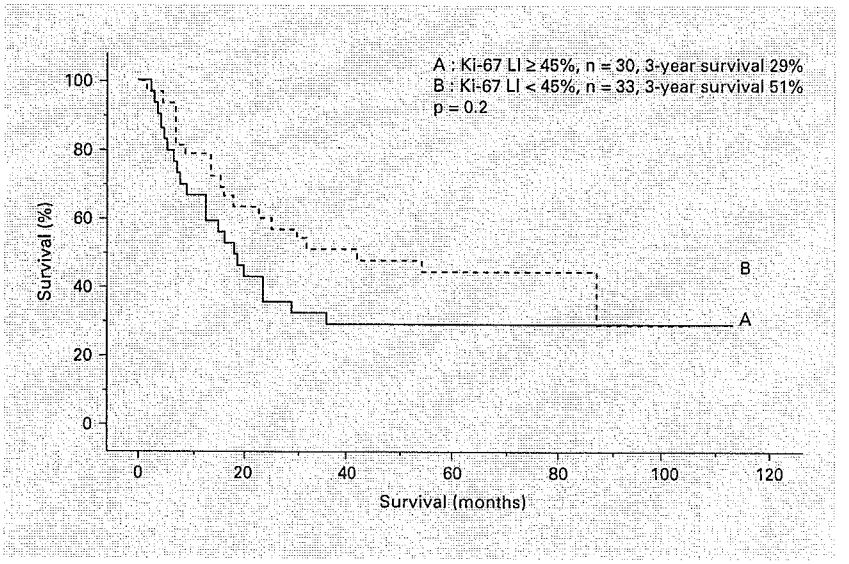

Fig. 6. Kaplan-Meier survival curves for patients with esophageal SCCs. Survival curves are stratified by Ki-67 LI. Ki-67 LI ≥ 45% represents high Ki-67 expression (A) and Ki-67 LI <45% low Ki-67 expression (B).

grade tumors than in moderate- to low-grade tumors ($p = 0.06$). Ki-67 LI was not associated with survival (3-year survival rate, 29% for patients having tumors with a high Ki-67 LI and 51% for patients having tumors with a low Ki-67 LI; $p = 0.2$) (fig. 6), and was not a significant prognostic factor in univariate analysis (table 2).

Discussion

This is the first study that examined GnT-V expression and its clinical significance in human normal, premalignant and malignant esophageal tissues. The present study demonstrates that GnT-V expression is found significantly more frequently in mildly and moderately dysplastic tissues when compared with normal epithelial and hyperplastic tissues, and when compared with in situ and invasive SCCs. Furthermore, GnT-V expression was frequently observed in SCCs of a small size and without distant metastasis or lymph node metastasis. These data suggest that GnT-V expression represents an early event in the development of human esophageal cancers, and that it may not be directly linked to tumor metastasis.

Previous studies demonstrated that high levels of GnT-V expression are correlated with a poor prognosis in human colorectal and breast cancers [15, 16]. On the other hand, expression of GnT-V in the liver is the early event in rat and human hepatocarcinogenesis [12, 18]. Ito et al. [18] reported that positive staining for GnT-V was observed in 60% of surrounding chronic hepatitis tissues, 71% of surrounding liver cirrhosis tissues, 100% of atypical adenomatous hyperplasias, and 75% of hepatocellular carcinomas (HCCs). Furthermore, high levels of GnT-V expression in HCCs were correlated with a low Ki-67 LI, small tumor size, and the absence of portal invasion. Levels of GnT-V expression in HCCs were not correlated with prognosis after surgery. These data in HCCs were similar to the present data in human esophageal SCCs. In addition, we recently found that low GnT-V expression is associated with shorter survival and poor prognosis in pStage I non-small cell lung cancers [26]. The different roles of GnT-V expression among various tumors, including esophageal SCCs, HCCs, non-small cell lung cancers, and colorectal and breast cancers, may be attributable at least partly to differences in the target proteins of GnT-V glycosylation [11, 27–29].

In the present study, the pattern of GnT-V expression did not overlap the staining pattern for β1,6-branched asparagine-linked oligosaccharides, as analyzed by L4-PHA histochemistry. We showed that β1,6-branched asparagine-linked oligosaccharides were found in the basal cell layers but not in the superficial cell layers in normal esophageal epithelium, and L4-PHA staining was observed in all of the 49 in situ and invasive SCCs examined. These results were consistent with previous studies [19, 20]. The discrepancy between L4-PHA staining and GnT-V expression could be attributed to several mechanisms, including expression of other enzymes synthesiz-

ing β1,6 branches and the levels of donor and acceptor substrate. A novel β1,6-N-acetylglucosaminyltransferase cDNA has recently been cloned and was designated GnT-IX by our group [30, 31] or GnT-VB by Pierce's group [32]. Moreover, it has been demonstrated that the in vivo levels of UDP-GlcNAc (donor substrate) are a critical factor for the production of β1,6 GlcNAc branching [33]. The amount of asparagine-linked oligosaccharides (acceptor substrate) is also important. In addition, the action of GnT-III prior to GnT-IV and GnT-V leads to the inhibition of multi-antennary oligosaccharides biosynthesis, because the bisecting N-acetylglucosamine (GlcNAc) moiety, catalyzed by GnT-III, does not serve as an acceptor substrate for α-mannnosidase II, or for GnT-II, GnT-IV, or GnT-V [34]. Thus, the formation of additional branching by GnT-V could be inhibited by the action of GnT-III.

Increased levels of β1,6 GlcNAc branching in human breast and colon carcinoma have previously been correlated with tumor development, invasion and metastasis [15, 16]. Li and Roth [19] reported that differentiated and nonmitotic epithelia in most organs showed strong lectin staining, and the exception was the epithelia of colon and resting mammary gland, which were unreactive to L4-PHA. Thus, an increase in L4-PHA staining intensity from normal epithelium to carcinoma seems to be present only in the colon and breast. The biological importance of this oligosaccharide structure in the regulatory function of normal epithelial cells and in the development, invasion and metastasis of cancer cells would vary in each organ. It is because target proteins of GnT-V could also be different in various cell types from different organs.

In the present study, we also studied Ki-67 LI in human esophageal SCCs. Ki-67 LI has been regarded as a parameter of cell proliferation [35], but a few studies [36, 37] have investigated Ki-67 cell proliferative activity in esophageal SCCs. Kawamura et al. [37] reported that Ki-67 LI was correlated with cancer invasion and lymph node metastasis in carcinomas with submucosal invasion. Our data showed that Ki-67 LI was strongly related to pT classification, pN classification and vascular invasion, and tended to be associated with lymphatic invasion and differentiation in SCCs. The present results were largely consistent with those of previous studies [36, 37].

In conclusion, increased expression of GnT-V was associated with the early event of esophageal tumorigenesis. While the presence of β1,6 GlcNAc branching was observed in SCCs, it was not correlated with GnT-V expression, suggesting that the regulation of β1,6 GlcNAc branching in esophageal SCCs could not be controlled by GnT-V alone.

Acknowledgement

We would like to thank Dr. Nobuichi Kasimura of the Teinekeijinkai Hospital and Dr. Takayuki Morita of the Hokkaido Gastroenterology Hospital for providing surgically resected specimens of esophageal cancers, Dr. Motoi Nishi of the Health Sciences University of Hokkaido for statistical analysis, and Dr. Noriko Okuyama and Dr. Kanako Yamanaka of the Osaka University Faculty of Medicine for Western and lectin blot analyses.

This work was supported in part by a Grant-in-Aid (No. 15659192) from the Ministry of Education, Science, Sports and Culture of Japan.

References

1 Ando N, Ozawa S, Kitagawa Y, Shinozawa Y, Kitajima M: Improvement in the results of surgical treatment of advanced squamous esophageal carcinoma during 15 consecutive years. Ann Surg 2000;232:225–232.

2 Adham M, Baulieux J, Mornex F, de La Roche de Bransat E, Ducerf C, Souquet JC, Gerard JP: Combined chemotherapy and radiotherapy followed by surgery in the treatment of patients with squamous cell carcinoma of the esophagus. Cancer 2000;89:946–954.

3 Collard JM, Otte JB, Fiasse RF, Laterre PF, De Knock M, Longueville J, Glineur D, Romagnoli R, Reynaert M, Kestens PJ: Skeletonizing en bloc esophagectomy for cancer. Ann Surg 2001;234:25–32.

4 Torres C, Turner JR, Wang HH, Richards W, Sugarbaker D, Shahsafaei A, Odze RD: Pathologic prognosis factors in Barrett's associated adenocarcinoma: a follow-up study of 96 patients. Cancer 1999;85:520–528.

5 Ando N, Iizuka T, Kakegawa T, Isono, K, Watanabe H, Ide H, Tanaka O, Shinoda M, Takiyama W, Arimori M, Ishida K, Tsugane S: A randomized trial of surgery with and without chemotherapy for localized squamous carcinoma of the thoracic esophagus: The Japan Clinical Oncology Group study. J Thorac Cardiovasc Surg 1997;114:205–209.

6 Rademacher TW, Parekh RB, Dwek RA: Glycobiology. Annu Rev Biochem 1988;57:785–838.

7 Hakomori S: Aberrant glycosylation in tumors and tumor-associated carbohydrate antigens. Adv Cancer Res 1989;52:257–331.

8 Cummings RD, Trowbridge IS, Kornfeld S: A mouse lymphoma cell line resistant to the leukoagglutinating lectin from *Phaseolus vulgaris* is deficient in UDP-GlcNAc:alpha-*D*-mannoside beta 1,6 N-acetylglucosaminyltransferase. J Biol Chem 1982;257:13421–13427.

9 Yamashita K, Tachibana I, Ohkura T, Kobata A: Enzymatic basis for the structure changes of asparagine-linked sugar chains of membrane glycoproteins of baby hamster kidney cells induced polyoma transformation. J Biol Chem 1985;260:3963–3969.

▶10 Pierce M, Arango J: Rous sarcoma virus-transformed baby hamster kidney cells express higher levels of asparagine-linked tri- and tetraantennary glycopeptides containing [GlcNAc-beta (1,6)Man-alpha (1,6)Man] and poly-N-acetyllactosamine sequences than baby hamster kidney cells. J Biol Chem 1986;261:10772–10777.

▶11 Demetriou M, Nabi IR, Coppolino M, Dedhar S, Dennis JW: Reduced contact-inhibition and substratum adhesion in epithelial cells expressing GlcNAc-transferase V. J Cell Biol 1995;130:383–392.

▶12 Miyoshi E, Nishikawa A, Ihara Y, Gu J, Sugiyama T, Hayashi N, Fusamoto H, Kamada T, Taniguchi N: N-Acetylglucosaminyltransferase III and V messenger RNA levels in LEC rats during hepatocarcinogenesis. Cancer Res 1993;53:3899–3902.

▶13 Seelentag WK, Li WP, Schmitz SF, Metzger U, Aeberhard P, Heitz PU, Roth J: Prognostic value of beta1,6-branched oligosaccharides in human colorectal carcinoma. Cancer Res 1998;58:5559–5564.

▶14 Granovsky M, Fata J, Pawling J, Muller WJ, Khokha R, Dennis JW: Suppression of tumor growth and metastasis in Mgat5-deficient mice. Nat Med 2000;6:306–312.

▶15 Dennis JW, Laferte S, Waghorne C, Breitman ML, Kerbel RS: Beta 1–6 branching of Asn-linked oligosaccharides is directly associated with metastasis. Science 1987;236:582–585.

▶16 Fernandes B, Sagman U, Auger M, Demetrio M, Dennis JW: Beta 1–6 branched oligosaccharides as a marker of tumor progression in human breast and colon neoplasia. Cancer Res 1991;51:718–723.

▶17 Murata K, Miyoshi E, Kameyama M, Ishikawa O, Kabuto T, Sasaki Y, Hiratsuka M, Ohigashi H, Ishiguro S, Ito S, Honda H, Takemura F, Taniguchi N, Imaoka S: Expression of N-acetylglucosaminyltransferase V in colorectal cancer correlates with metastasis and poor prognosis. Clin Cancer Res 2000;6:1772–1777.

▶18 Ito Y, Miyoshi E, Sakon M, Takeda T, Noda K, Tsujimoto M, Ito S, Honda H, Takemura F, Wakasa K, Monden M, Matsuura N, Taniguchi N: Elevated expression of UDP-N-acetylglucosamine: alphamannoside beta1,6 N-acetylglucosaminyltransferase is an early event in hepatocarcinogenesis. Int J Cancer 2001;91:631–637.

▶19 Li WP, Roth J: Expression of beta 1,6 branched asparagine-linked oligosaccharides in non-mitotic and non-migratory cells of normal human and rat tissues. Int J Cancer 1997;71:483–490.

▶20 Takano R, Nose M, Nishihira T, Kyogoku M: Increase of beta 1-6-branched oligosaccharides in human esophageal carcinomas invasive against surrounding tissue in vivo and in vitro. Am J Pathol 1990;137:1007–1011.

21 International Union Against Cancer: TNM Classification of Malignant Tumours, ed 6. New York, Wiley-Liss, 2002, pp 60–64.

▶22 Cummings RD, Kornfeld S: Characterization of the structural determinants required for the high affinity interaction of asparagine-linked oligosaccharides with immobilized *Phaseolus vulgaris* leukoagglutinating and erythroagglutinating lectins. J Biol Chem 1982;257:11230–11234.

▶23 Miyoshi E, Ihara Y, Hayashi N, Fusamoto H, Kamada T, Taniguchi N: Transfection of N-acetylglucosaminyltransferase III gene suppresses expression of hepatitis B virus in a human hepatoma cell line, HB611. J Biol Chem 1995;270:28311–28315.

▶24 Gerdes J, Schwab U, Lemke H, Stein H: Production of a mouse monoclonal antibody reactive with a human nuclear antigen associated with cell proliferation. Int J Cancer 1983;31:13–20.

▶25 Ishikuro A, Dosaka-Akita H, Kato M, Fujino M, Isobe H, Miyamoto H, Inoue K, Kawakami Y: Ki-67 labeling indices in non-small cell lung cancer: comparison between image cytometry and flow cytometry. Cytometry 1997;30:186–191.

▶26 Dosaka-Akita H, Miyoshi E, Suzuki O, Itoh T, Katoh H, Taniguchi N: Expression of N-acetylglucosaminyltransferase v is associated with prognosis and histology in non-small cell lung cancers. Clin Cancer Res 2004;10:1773–1779.

▶27 Guo HB, Lee I, Kamar M, Akiyama SK, Pierce M: Aberrant N-glycosylation of beta1 integrin causes reduced alpha5beta1 integrin clustering and stimulates cell migration. Cancer Res 2002;62:6837–6845.

▶28 Ihara S, Miyoshi E, Ko JH, Murata K, Nakahara S, Honke K, Dickson RB, Lin CY, Taniguchi N: Prometastatic effect of N-acetylglucosaminyltransferase V is due to modification and stabilization of active matriptase by adding beta 1-6 GlcNAc branching. J Biol Chem 2002;277:16960–16967.

▶29 Saitoh O, Wang WC, Lotan R, Fukuda M: Differential glycosylation and cell surface expression of lysosomal membrane glycoproteins in sublines of a human colon cancer exhibiting distinct metastatic potentials. J Biol Chem 1992;267:5700–5711.

▶30 Inamori K, Endo T, Ide Y, Fujii S, Gu J, Honke K, Taniguchi N: Molecular cloning and characterization of human GnT-IX, a novel beta1,6-N-acetylglucosaminyltransferase that is specifically expressed in the brain. J Biol Chem 2003;278:43102–43109.

▶31 Inamori K, Endo T, Gu J, Matsuo I, Ito Y, Fujii S, Iwasaki H, Narimatsu H, Miyoshi E, Honke K, Taniguchi N: N-Acetylglucosaminyltransferase IX acts on the GlcNAc beta 1,2-Man alpha 1-Ser/Thr moiety, forming a 2,6-branched structure in brain O-mannosyl glycan. J Biol Chem 2004;279:2337–2340.

▶32 Kaneko M, Alvarez-Manilla G, Kamar M, Lee I, Lee JK, Troupe K, Zhang W, Osawa M, Pierce M: A novel beta(1,6)-N-acetylglucosaminyltransferase V (GnT-VB)(1). FEBS Lett 2003;554:515–519.

▶33 Sasai K, Ikeda Y, Fujii T, Tsuda T, Taniguchi N: UDP-GlcNAc concentration is an important factor in the biosynthesis of beta1,6-branched oligosaccharides: regulation based on the kinetic properties of N-acetylglucosaminyltransferase V. Glycobiology 2002;12:119–127.

▶34 Sasai K, Ikeda Y, Eguchi H, Tsuda T, Honke K, Taniguchi N: The action of N-acetylglucosaminyltransferase-V is prevented by the bisecting GlcNAc residue at the catalytic step. FEBS Lett 2002;522:151–155.

▶35 Sasaki K, Murakami T, Kawasaki M: The cell cycle associated change of the Ki-67 reactive nuclear antigen expression. J Cell Physiol 1987;133:579–584.

▶36 Lam KY, Law SY, So MK, Fok M, Ma LT, Wong J: Prognostic implication of proliferative markers MIB-1 and PC10 in esophageal squamous cell carcinoma. Cancer 1996;77:7–13.

▶37 Kawamura T, Goseki N, Koike M, Takizawa T, Endo M: Acceleration of proliferative activity of esophageal squamous cell carcinoma with invasion beyond the mucosa: immunohistochemical analysis of Ki-67 and p53 antigen in relation to histopathologic findings. Cancer 1996;77:843–849.

E1AF/PEA3 Activates the Rho/Rho-Associated Kinase Pathway to Increase the Malignancy Potential of Non–Small-Cell Lung Cancer Cells

Nobuyuki Hakuma,[1] Ichiro Kinoshita,[2] Yasushi Shimizu,[2] Koichi Yamazaki,[1] Koichi Yoshida,[3] Masaharu Nishimura,[1] and Hirotoshi Dosaka-Akita[2]

[1]First Department of Medicine and [2]Department of Medical Oncology, Hokkaido University Graduate School of Medicine and [3]Department of Biology, Sapporo Medical University School of Medicine, Sapporo, Japan

Abstract

E1AF/PEA3, an Ets family transcription factor, is frequently overexpressed in non–small-cell lung cancers (NSCLCs). Overexpression of E1AF increases motility and invasion of VMRC-LCD and NCI-H226 NSCLC cells, which lack endogenous E1AF expression, and the effect is synergistically increased by hepatocyte growth factor (HGF). The small GTPase Rho/Rho-associated kinase (ROCK) pathway is also involved in motility and invasion. To determine the role of the Rho/ROCK pathway in malignant phenotypes induced by E1AF, we analyzed VMRC-LCD cells transfected with an E1AF expression vector (LCD-E1AF cells) or with empty vector (LCD-vector cells). LCD-E1AF cells had more GTP-bound (active) Rho than LCD-vector cells and Rho activation was synergistically increased by HGF. The Rho activation by E1AF and HGF was also shown in NCI-H226 cells. Phosphorylation of myosin light chain (MLC), a downstream effector of ROCK signaling, was higher in LCD-E1AF cells than in LCD-vector cells, especially under HGF treatment. A specific ROCK inhibitor, Y27632, strongly suppressed MLC phosphorylation, cell motility, and invasion. In nude mice implanted s.c. and intrapulmonarily, LCD-E1AF cells made more local tumors than LCD-vector cells (six of six versus one of seven mice and four of seven versus one of seven mice, respectively). Three of the four mice with lung tumors from LCD-E1AF cells had lymph node metastases whereas the mouse with LCD-vector tumors did not. LCD-E1AF tumors showed higher MLC phosphorylation than LCD-vector tumors. These results suggest that E1AF activates the Rho/ROCK pathway in an HGF-enhanced manner and its activation is important in E1AF-induced motility and invasion as well as tumorigenesis and metastasis in NSCLC cells. (Cancer Res 2005; 65(23): 10776-82)

Introduction

Cell motility and invasion as well as tumorigenesis and metastasis characterize the malignancy potential of cancer. Members of the Ets-related oncoprotein family are transcription factors with a highly conserved ETS domain; they play important roles in the regulation of gene expression during such biological processes as oncogenesis (1). One Ets-related family member, E1AF (2), a human homologue of mouse PEA3 (3), was isolated by its ability to bind adenovirus E1A enhancer elements. E1AF can up-regulate transcription from several subclasses of matrix metalloproteinase (MMP) genes in transient expression assays (2). Expression of E1AF confers an invasive phenotype on MCF7, a human breast cancer cell line (4). E1AF expression is correlated with the transcription of MMPs and the invasive phenotype in oral squamous cell carcinoma cell lines (5). We have previously reported that E1AF is frequently overexpressed in non–small-cell lung cancers (NSCLC) and its expression increases motility and invasion of NSCLC cell lines VMRC-LCD and NCI-H226, which normally lack E1AF expression (6). In addition, recent *in vivo* experiments show that E1AF increases the metastatic activity of fibrosarcoma cells through expression of membrane type 1 MMP (7) and that mammary oncogenesis induced by HER2/neu is strongly inhibited by blockade of E1AF (8). These observations suggest the E1AF has roles in various malignant phenotypes of cancer cells but the mechanisms remain to be discovered.

Rho, a well-known member of the p21 Ras superfamily of small GTPases, exhibits both GDP/GTP binding and GTPase activities. Rho serves as a molecular switch, regulating signal transduction from receptors in the membrane to various cellular events related to cell morphology (9), motility (10), cytoskeletal dynamics (11, 12), and tumor progression (13, 14; for reviews, see refs. 15–17). Rho activates Rho-associated kinase (ROCK), which then increases phosphorylation of myosin light chain (MLC; ref. 18). Phosphorylated MLC induces the contraction of myosin and subsequently organizes the actin stress fibers and focal adhesions. Activation of Rho/ROCK signaling is also known to stimulate the organization of actin stress fibers and to enhance the motility and invasion of rat hepatoma cells (19, 20), human glioma cells (21), and human ovarian cancer cells (22). Recently, studies using clinical specimens showed a relationship between the expression level of RhoC, an isoform of Rho, and tumor aggressiveness in breast cancer (23–25), pancreatic cancer (26), and NSCLCs (27). Furthermore, RhoC also enhances metastasis of melanoma cells (28) and lung cancer cells (29) in mouse model systems.

To determine whether the Rho/ROCK pathway is involved in E1AF-associated malignant phenotypes in NSCLCs, we examined E1AF- and vector-transfected VMRC-LCD NSCLC cells for Rho activity and its relation to motile and invasive activities. To increase the effects of E1AF, we used hepatocyte growth factor (HGF), a strong cell-scattering factor that is frequently overexpressed in various human cancers including NSCLCs. We have shown that HGF acts synergistically with E1AF to increase motile and invasive activities in VMRC-LCD cells (6). We treated the cells with a specific ROCK inhibitor, Y27632 (20), to determine whether activation of the Rho/ROCK pathway is required for

Requests for reprints: Ichiro Kinoshita, Department of Medical Oncology, Hokkaido University Graduate School of Medicine, North 15, West 7, Kita-ku, Sapporo 060-8638, Japan. Phone: 81-11-706-5551; Fax: 81-11-706-5077; E-mail: kinoshii@med.hokudai.ac.jp.

doi:10.1158/0008-5472.CAN-05-0060

the enhancement of motile and invasive activities by E1AF. Furthermore, we examined E1AF- and vector-transfected cells for tumorigenic and metastatic activities *in vivo* and their relationship with phosphorylation of MLC, a downstream effector of ROCK.

Materials and Methods

Cell lines and cell culture. VMRC-LCD and A549 NSCLC cell lines were obtained from the Health Science Research Resource Bank of Japan (Osaka, Japan). NCI-H226 and NCI-H520 NSCLC cell lines were kindly provided by Dr. H. Oie (Navy Medical Oncology Branch, National Cancer Institute, Bethesda, MD). All cell lines were cultured in RPMI 1640 supplemented with 10% fetal bovine serum (FBS) and 0.03% glutamine at 37°C in an atmosphere of 5% CO_2. LCD-E1AF cells (VMRC-LCD cells transfected with the E1AF-expression vector pCMV-E1AF and pRSVneo), LCD-vector control cells (VMRC-LCD cells transfected with the empty vector pEV3S and pRSVneo), H226-E1AF cells (NCI-H226 cells transfected with the E1AF-expression vector pCMV-E1AF and pRSVneo), and H226-vector control cells (H226 cells transfected with the empty vector pEV3S and pRSVneo) have been described in our previous article (6). Although not stated in that article, they were pools of G418-resistant cells consisting of at least 100 independent clones, which could minimize possible clonal variations. The established cells had been stocked in aliquots in liquid nitrogen until experiments were started. Only cells in early passages were used for the experiments to avoid molecular changes during prolonged period of culture.

pLNTK-E1AF–infected SiHa cells were cultured in DMEM supplemented with 10% FBS and 0.03% glutamine at 37°C in an atmosphere of 5% CO_2 and used for positive control for Western blot analysis of E1AF protein (30).

Western blot analysis of E1AF. Western blot analyses of E1AF were done as previously described (30). Briefly, purified total protein (30 μg) from isolated subconfluent cells was separated by SDS-PAGE, transferred to nitrocellulose membranes, and reacted with an anti-E1AF monoclonal antibody (a gift from Dr. Chono, Takara Bio, Otsu, Japan). The primary antibody was detected using an antirabbit antibody conjugated with horseradish peroxidase and visualized by the Amersham enhanced chemiluminescence (ECL) system (Amersham, Arlington Heights, IL). pLNTK-E1AF–infected SiHa cells were used for positive control of E1AF protein expression (30). The same lysates were used in Western blotting of actin as an internal control.

***In vitro* motility and invasion assays.** Transwell cell culture chambers (pore size, 8 μm; Costar, Cambridge, MA) were used for the motility and invasion assays. For the motility assay, 1×10^5 LCD-E1AF and LCD-vector cells were suspended in serum-free RPMI 1640 with 0.1% bovine serum albumin (BSA; Sigma Chemical, St. Louis, MO) and added to the upper chamber. The reverse side of the upper chamber filter was coated with 10 μg human cellular fibronectin (Biomedical Technologies, Stoughton, MA) as a chemoattractant. Serum-free RPMI 1640 with 0.1% BSA was added to the lower chamber. For the invasion assay, 2×10^5 LCD-E1AF and LCD-vector cells were suspended in serum-free RPMI 1640 with 0.1% BSA and added to the upper chamber. The upper chamber filter was coated with 10 mg mouse Matrigel (Becton Dickinson Labware, Franklin Lakes, NJ) and the reverse side of the upper chamber filter was coated with 10 μg human cellular fibronectin as a chemoattractant. Serum-free RPMI 1640 with 0.1% BSA was added to the lower chamber. In both motility and invasion assays, a specific ROCK inhibitor, Y27632 (0, 1, 10, or 100 μmol/L; Calbiochem, Darmstadt, Germany), was added to the upper and lower chambers and HGF (40 ng/mL; Toyobo, Osaka, Japan) was added to the lower chamber as indicated. These cells were incubated at 37°C in an atmosphere of 5% CO_2 for 24 hours for both motility and invasion assays.

Cell growth assay. Cell growth was measured using an assay based on 3-(4,5-dimethylthiazol-2-yl)-2,5-diphenyltetrazolium bromide (MTT; non-radioactive proliferation assay, Promega, Madison, WI). Cells (1×10^4) in 0.1 mL of RPMI 1640 with 10% FBS or 0.1% BSA, with or without 100 μmol/L Y27632, were seeded onto each well of 96-well plates and then incubated at 37° C in an atmosphere of 5% CO_2 for 1, 3, or 5 days. To each well was added 15 μL of Dye Solution (Promega) and then cells were incubated at 37° C for 4 hours. After 4 hours, 100 μL of Solubilization/Stop Mix solution (Promega) were added to each well. One hour later, the contents of the wells were mixed to yield a uniformly colored solution. The absorbance at 590 nm was recorded using a 96-well plate reader and the survival fraction was quantified.

Rho pull-down assay. The Rho pull-down assay was done as previously described (31). Briefly, cells (3.5×10^5/mL) were plated and cultured under 10% serum conditions with or without HGF for 24 hours. After incubation, cells were washed twice with PBS and lysed in Laemmli's SDS sample buffer (32). Cell lysates were clarified by centrifugation. For controls, LCD-vector cell lysate or H226-vector cell lysate containing 1.5 mg total protein was incubated at 30°C for 30 minutes with 100 μmol/L GTP-γS (Upstate Biotechnology, Lake Placid, NY) for the positive control or with 100 μmol/L GDP (Upstate Biotechnology) for the negative control. Cell lysates containing 1.5 mg total protein were incubated with 30 μg Rhotekin RBD-agarose beads (Upstate Biotechnology) at 4°C for 45 minutes. The beads were washed thrice with PBS. GTP-bound Rho proteins were detected by Western blotting using a polyclonal antibody against Rho (RhoA, RhoB, and RhoC; Upstate Biotechnology) overnight at 4°C. The primary antibodies

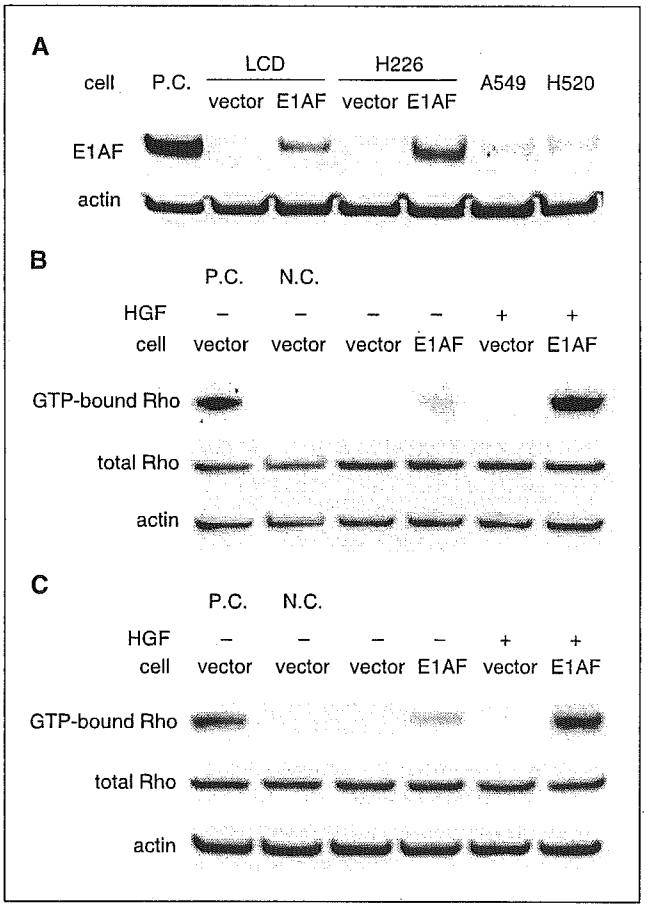

Figure 1. Rho activation by E1AF in NSCLC cells. *A*, Western blot analysis of E1AF protein of LCD-vector and LCD-E1AF cells, H226-vector and H226-E1AF cells, and A549 and NCI-H520 cells. *P.C.*, positive control (pLNTK-E1AF–infected SiHa cells; ref. 30). *B*, Western blot analysis of intracellular levels of GTP-bound Rho and total Rho in LCD-vector and LCD-E1AF cells. For GTP-bound (active) Rho, total protein isolated from cells cultured for 24 hours, with or without HGF (40 ng/mL), was incubated with Rhotekin RBD-agarose beads to bind active Rho. Then GTP-bound Rho was detected by Western blotting using an anti-Rho (RhoA, RhoB, and RhoC) polyclonal antibody. *N.C.*, negative control (see Materials and Methods). The same lysates were used in Western blotting of total Rho and actin as an internal control for the comparison of levels of GTP-bound Rho. *C*, same experiments as in (*B*) were done using H226-vector and H226-E1AF cells.

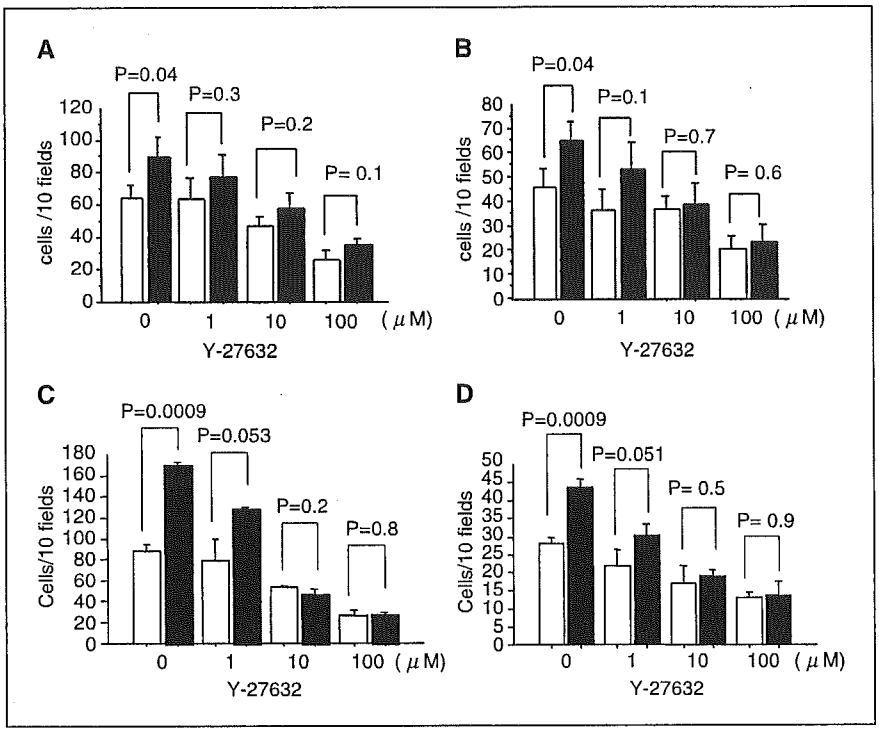

Figure 2. *In vitro* motility and invasion of LCD-vector (*open columns*) and LCD-E1AF (*closed columns*) cells with various concentrations of Y27632. Cells were incubated for 24 hours with various concentrations of Y27632, with or without HGF treatment (40 ng/mL), and the number of migrated cells was counted at a magnification of ×200. *A* and *B*, motility assay (*A*) and invasion assay (*B*) without HGF; *C* and *D*, motility assay (*C*) and invasion assay (*D*) with HGF. *Columns*, mean; *bars*, SD.

were detected using anti-rabbit antibody conjugated with horseradish peroxidase and visualized with the Amersham ECL system. The same lysates were used in Western blotting of total Rho and actin as an internal control for the comparison of levels of GTP-bound Rho.

Western blot analysis of myosin light chain. LCD-E1AF and LCD-vector cells were cultured in RPMI 1640 with 10% FBS for 24 hours, then with or without 40 ng/mL HGF, and finally with 100 μmol/L Y27632 for 0, 1, 4, 8, 12, and 24 hours. Cells were washed twice with PBS and lysed in ice-cold lysis buffer [10 mmol/L Tris (pH 7.4), 150 mmol/L NaCl, 1% Triton X-100, 0.1% deoxycholate, 0.1% SDS, 100 μg/mL leupeptin, 100 μg/mL aprotinin, and 1 mmol/L phenylmethylsulfonyl fluoride]. Cell lysates containing 30 μg total protein were separated on SDS-polyacrylamide gels, transferred to nitrocellulose membrane, and then reacted with anti-MLC antibody from mice (Sigma Chemical) or anti–phosphorylated MLC antibody from rabbits (Cell Signaling, Beverly, MA). The primary antibodies were detected using antimouse or antirabbit antibody conjugated with horseradish peroxidase and visualized with the Amersham ECL system.

Mice. Female BALB/c athymic nude mice, 4 to 6 weeks old, were purchased from Clea Japan, Inc. (Tokyo, Japan) and maintained in a specific pathogen-free environment throughout the experiment.

Tumor implantation. LCD-E1AF or LCD-vector cells (1×10^7) were injected i.v. into the tail vein or s.c. into the flank of 6- to 8-week-old nude mice. The mice injected s.c. were examined for localized tumor and for metastasis to mediastinal lymph node, liver, kidney, and spleen. The weight of each tumor was measured.

The implantation of LCD-E1AF and LCD-vector cells into the lung was done as previously described (33) with some modifications. Briefly, the left chest of each anesthetized mouse was incised (~5 mm incision) just below the inferior border of the scapula, and 20 μL of suspension containing 1×10^7 VMRC-LCD cells and 20 μg of Matrigel were injected into the left lung parenchyma through the intercostal space. The skin incision was closed with 3-0 silk. Mice were sacrificed on days 14, 28, and 42 after tumor cell implantation. Tumors were examined in lung, mediastinal lymph node, liver, kidney, and spleen and were weighed.

Histologic examination. The sacrificed mice were examined and then the tumors in the lungs and mediastinal lymph nodes were removed and weighed. After careful macroscopic examination, tumors were fixed with 10% formalin, embedded in paraffin, cut into 4-μm sections, and then stained with H&E.

Western blot analysis of mouse tumor homogenates. Single s.c. tumor from a mouse implanted with LCD-vector cells or a mouse with LCD-E1AF cells, single lung tumor from a mouse with LCD-vector cells, a pool of lung tumors from five mice with LCD-E1AF cells, and a pool of mediastinal lymph node tumors from four mice with LCD-E1AF cells were homogenized and sonicated in 1.0 mL of ice-cold lysis buffer. Specimens were centrifuged at 900 × *g* for 15 minutes and supernatants were filtered through sterile filters of 10 μm pore size (Toyo Roshi, Tokyo, Japan). Cell lysates containing 30 μg total protein were separated on SDS-polyacrylamide gels, transferred to nitrocellulose membrane, and then reacted with anti-MLC antibody from

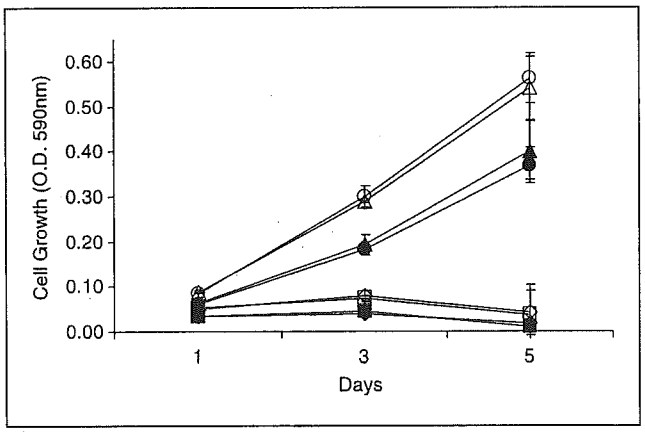

Figure 3. Effect of Y27632 on VMRC-LCD cell growth. Cells were cultured with or without 100 μmol/L Y27632 and with 10% FBS or 0.1% BSA. Cell growth was analyzed by MTT assay. ○, LCD-vector in FBS without Y27632; △, LCD-vector in FBS with Y27632; ●, LCD-E1AF in FBS without Y27632; ▲, LCD-E1AF in FBS with Y27632; □, LCD-vector in BSA without Y27632; ◇, LCD-vector in BSA with Y27632; ■, LCD-E1AF in BSA without Y27632; ♦, LCD-E1AF in BSA with Y27632. *Points*, mean; *bars*, SD.

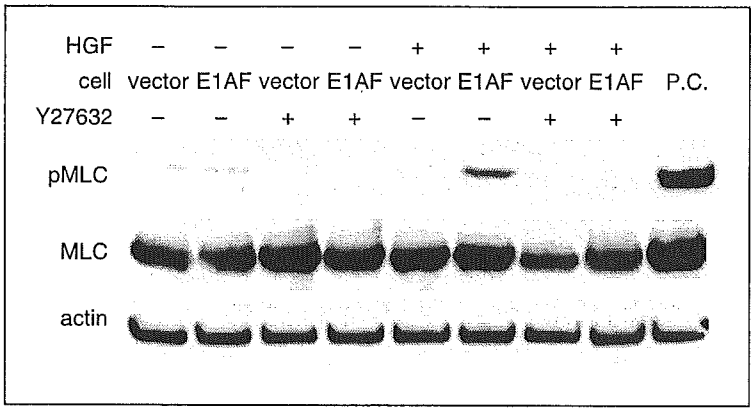

Figure 4. Western blot analysis of intracellular phosphorylated MLC, total MLC, and actin in LCD-vector and LCD-E1AF cells. Total protein was isolated from subconfluent cells cultured with or without HGF (40 ng/mL) for 24 hours and with or without Y27632 (100 μmol/L) for 24 hours. Levels of phosphorylated MLC and total MLC were determined by Western blot analysis. The protein from the lung tumors of E1AF cells in Fig. 5 was also used in this figure for positive control.

mice and anti–phosphorylated MLC antibody from rabbits. The primary antibodies were detected using antimouse or antirabbit antibody conjugated with horseradish peroxidase and visualized with the Amersham ECL system.

Statistical analysis. Statistical differences in the means were examined by Student's unpaired two-tailed *t* test.

Results

E1AF activates Rho in VMRC-LCD cells. We have previously reported frequent overexpression of E1AF in NSCLC cell lines, except for VMRC-LCD and NCI-H226 cells, using Northern blot analysis and generation of E1AF-expressing VMRC-LCD and NCI-H226 cells (6). Western blot analysis using an anti-E1AF monoclonal antibody confirmed the presence of E1AF protein expression in LCD-E1AF and H226-E1AF cells and the absence of endogenous E1AF protein in LCD-vector and H226 vector cells (Fig. 1*A*). Endogenous E1AF protein expression was detected in A549 and NCI-H520 cells whereas it was weaker than that in LCD-E1AF and H226-E1AF cells.

To determine the effect of E1AF expression on Rho activity in VMRC-LCD, we measured the intracellular levels of GTP-bound (active) Rho using a pull-down assay system. We compared the activity of Rho in LCD-E1AF cells and LCD-vector cells with and without HGF treatment. As shown in Fig. 1*B*, the level of the GTP-bound (active) Rho was higher in LCD-E1AF cells than in LCD-vector cells. HGF enhanced the level of active Rho strongly in LCD-E1AF cells but had little effect in LCD-vector cells. Total Rho protein levels were similar under each condition in each cell line (Fig. 1*B*), showing that the activation was not caused by an increase in Rho expression.

We did the same experiments using H226-E1AF and H226-vector cells (Fig. 1*C*) as in LCD-E1AF and LCD-vector cells. H226-E1AF cells also showed higher active Rho levels than H226-vector cells in a HGF-enhanced manner whereas total Rho protein was similar between the cells, suggesting that the activation of Rho protein by E1AF and HGF without an increase in its expression is not due to variation in NSCLC cell lines.

A Rho-associated kinase inhibitor decreases cell motility and invasion. We next determined the effects of Y27632, a small-molecule inhibitor of ROCK. As in our previous report (6), LCD-E1AF cells showed significantly more motile and invasive activities than LCD-vector cells (motility, $P = 0.04$; invasion, $P = 0.04$; Fig. 2*A* and *B*) especially under HGF treatment (motility, $P = 0.009$; invasion, $P = 0.009$; Fig. 2*C* and *D*). Y27632 dose-dependently inhibited motility and invasion in both cell lines and at high Y27632 concentration, these activities became similarly low (Fig. 2), indicating that Y27632 decreased the motile and invasive activities more in LCD-E1AF cells than in LCD-vector cells.

To assess whether Y27632 was toxic, MTT assays were done with or without 10% serum. As shown in Fig. 3, Y27632 at 100 μmol/L, the highest concentration used in Fig. 2, did not affect the growth of either VMRC-LCD cell line with or without serum.

E1AF increases phosphorylation of myosin light chain whereas a Rho-associated kinase inhibitor decreases its phosphorylation. To analyze the effect of E1AF on ROCK activity in VMRC-LCD cells, we measured the phosphorylation of MLC,

Table 1. Tumorigenic and metastatic activities of LCD-vector and LCD-E1AF cells after s.c. and intrapulmonary implantation in nude mice

	S.c. implantation (day 56)		Intrapulmonary implantation (day 42)	
	Primary*	Metastasis*	Primary*	Metastasis*
LCD-vector	1/7 (0.23 ± 0.62 g)†	0/6	1/7 (9 ± 23 mg)‡	0/6
LCD-E1AF	6/6 (4.73 ± 3.29 g)†	0/6	4/7 (66 ± 65 mg)‡	3/7 (71 ± 92 mg)§

*Data are shown as no. of mice with tumor/no. of total mice (tumor weight per mouse shown as mean ± SD).
†$P < 0.01$, LCD-E1AF versus LCD-vector.
‡$P < 0.05$, LCD-E1AF versus LCD-vector.
§Metastatic site of all three mouse was mediastinal lymph node.

a downstream effector of ROCK, using Western blot analysis. As shown in Fig. 4, phosphorylated MLC was more abundant in LCD-E1AF cells than in LCD-vector cells. HGF strongly enhanced the phosphorylation of MLC in LCD-E1AF cells but not in LCD-vector cells. Y27632 inhibited the phosphorylation of MLC induced by E1AF and HGF to an undetectable level.

E1AF increases tumorigenic and metastatic activities in association with phosphorylated myosin light chain. The tumorigenicity and metastasis potential of LCD-E1AF and LCD-vector cells was investigated by injection into nude mice. Eight weeks after i.v. injection of LCD-E1AF or LCD-vector cells, no tumor was observed in any organs (data not shown). After s.c. injection, all of six mice injected with LCD-E1AF cells and one of seven mice injected with LCD-vector cells had local tumors in flank subcutis 56 days after transplantation (Table 1). The s.c. tumors of LCD-E1AF cells were significantly heavier than those of LCD-vector (4.73 ± 3.29 versus 0.23 ± 0.62 g, $P < 0.005$). No metastatic tumors were observed in any organs from either cell line. When intrapulmonarily injected, LCD-E1AF and LCD-vector cells formed local tumors in the lung in four of seven and one of seven nude mice, respectively, 42 days after transplantation (Table 1). Each tumor-bearing mouse had one lung tumor. Lung tumors of LCD-E1AF cells were significantly heavier than those of LCD-vector (66 ± 65 versus 9 ± 23 mg, $P < 0.05$). Metastatic tumors from LCD-E1AF cells were observed in mediastinal lymph nodes in three of the four mice with lung tumors at 42 days (Fig. 5*A*). The number of mediastinal metastasis was three for one mouse at 42 days and one for the other three mice. The mean tumor weight was 71 ± 92 mg at 42 days after transplantation. Histopathologic examinations confirmed adenocarcinoma occupying the mediastinal lymph node (Fig. 5*B*). In contrast, there was no metastasis in mediastinal lymph nodes from the mouse with lung tumors of LCD-vector cells. There were no metastases from tumors of either cell line in the other organs.

To test whether Rho/ROCK signal is activated by E1AF *in vivo*, we examined the phosphorylation of MLC in tumors developed from LCD-E1AF and LCD-vector cells. By Western blot analysis (Fig. 5*C*), phosphorylated MLC was much more abundant in s.c., lung, and mediastinal lymph node tumors from LCD-E1AF cells than in s.c. and lung tumors from LCD-vector cells.

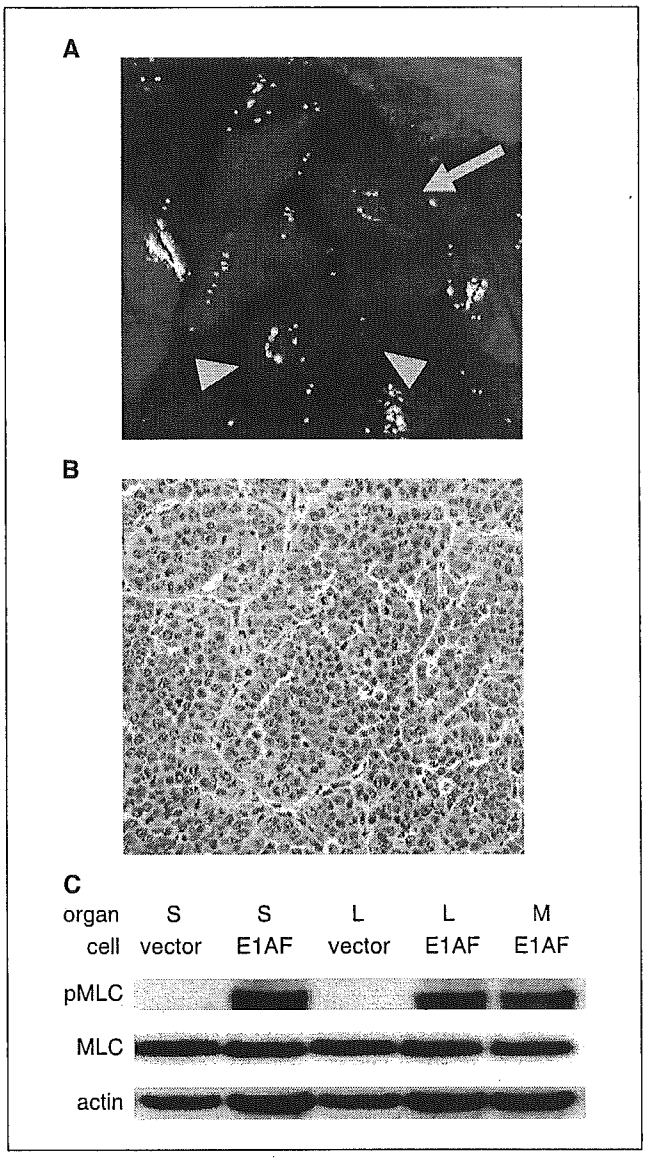

Figure 5. *In vivo* tumorigenic and metastatic activities of LCD-E1AF cells. *A*, tumor growth 42 days after intrapulmonary implantation of LCD-E1AF cells in nude mice. LCD-E1AF cells (1×10^7) were injected into the left lung parenchyma through the intercostal space. Tumors were observed in the lung (*arrow*) and in mediastinal lymph nodes (*arrowhead*). *B*, histopathologic examinations of the metastatic tumors in mediastinal lymph nodes confirmed adenocarcinoma occupying the mediastinal lymph node (magnification, ×400). *C*, Western blot analysis of phosphorylated MLC in tumors developed from LCD-E1AF and LCD-vector cells. S.c. (*S*), lung (*L*), and mediastinal lymph node (*M*) tumors from mice were homogenized and sonicated, and then total proteins (30 μg) purified from the tumors were separated on SDS-polyacrylamide gels, transferred to nitrocellulose membrane, and reacted with anti-MLC antibody, anti–phosphorylated MLC antibody, or anti-actin antibody as control. For lung and mediastinal tumors of LCD-E1AF cells, multiple tumors from the same tumor-bearing mice were pooled for these analyses (see Materials and Methods).

Discussion

This is the first study showing that E1AF overexpression results in the activation of the Rho/ROCK signaling pathway. HGF accentuated this activation strongly. The inhibition of cell migration and invasion by a ROCK inhibitor suggests that Rho/ROCK activation is necessary for cell migration and invasion induced by E1AF. Furthermore, we have shown an increase in tumorigenesis and metastasis caused by E1AF expression, which also results in phosphorylation of MLC, a downstream target of Rho/ROCK signaling.

We have previously shown that E1AF increases migration and invasion of cancer cells and that the increased invasion is associated with E1AF-induced expression of MMPs and urokinase plasminogen activator (uPA; refs. 2, 4–6). In this study, we have shown abundant GTP-bound Rho in E1AF-transfected cells, suggesting that another mechanism, the activation of Rho, may be involved in migration and invasion enhanced by E1AF. Extensive studies have shown that increased motility and invasion induced by Rho are mediated through its downstream molecules, ROCK and MLC (15–18); MLC phosphorylation was shown in E1AF-transfected cells in the present study. Furthermore, a specific ROCK inhibitor, Y27632, inhibited cell migration and motility and decreased phosphorylation of MLC, suggesting that activation of Rho/ROCK signaling is necessary for E1AF-induced migration and invasion.

The Rho/ROCK signaling pathway has been shown to be involved in motility and invasion of various cancer cell lines, such as rat

hepatoma cells (20), human glioma cells (21), and human ovarian cancer cells (22). Studies using clinical specimens showed a relationship between the expression level of RhoC, an isoform of Rho, and tumor aggressiveness in breast cancer (23–25) and pancreatic cancer (26). Recently, NSCLCs have also been shown to express RhoC mRNA and protein at higher levels than do nontumor tissues, and the RhoC expression level is correlated to vascular permeation (27). Taken together with the accumulating data showing association of Rho/ROCK signaling with migration and invasion, the present results suggest that the Rho/ROCK signaling has a central role in migration and invasion enhanced by E1AF in NSCLC cells.

E1AF has previously been correlated with altered expression of several genes, including *uPA*, *MMP*, and another Ets family gene, *Ets-1* (2, 6). LCD-E1AF cells were found to overexpress Ets-1 and the kinetics of HGF-mediated activation of Ets-1 is better correlated with uPA level than with E1AF level (6). This may suggest that the biological changes in the cell line may be mediated by altered expression of Ets-1 or possibly other Ets family members. All of ~30 Ets family transcription factors bind GGAA/T core sequence with some specificity depending on flanking sequences, suggesting their redundant functions (34). To determine their involvement in the phenotypes of E1AF-overexpressing cells, experiments with small interfering RNA of Ets-1 and other Ets family members possibly overexpressed in the cells will be required.

To our knowledge, the relationship of not only E1AF but also of other Ets family members, including Ets-1, with the activation of Rho has not been previously reported. Although E1AF and Ets-1 are transcription factors, their expression did not increase total Rho protein, suggesting that the activation of Rho is not caused by their transcriptional regulation. Rho activity is regulated by guanine nucleotide exchange factors (GEF) and GTPase activating proteins (GAP; ref. 35). Possible mechanisms for the Rho activation by E1AF include transcriptional regulation of GEFs and GAPs directly by E1AF or indirectly by potential mediators like Ets-1. A growing number of GEFs and GAPs for the Rho family have been identified, which by now include 69 Dbl-related GEF proteins, the largest family of RhoGEF, and more than 30 RhoGAPs (36, 37). To determine whether the activation of Rho by E1AF involves such mechanisms, comprehensive analyses including microarray analysis should be investigated in the near future.

The detection of endogenous E1AF protein in A549 and NCI-H520 cells is consistent with our previous study showing the E1AF mRNA expression in these cells and suggests roles of the endogenous E1AF protein in NSCLC cell lines. Loss of function studies of E1AF in the E1AF-expressing cell lines would clarify the roles of E1AF in the observed phenotypes, including Rho signaling activation, especially in a physiologic context.

The tumorigenicity potential of E1AF is indicated by the observed increase in incidence and weight of tumors in the skin and lung of nude mice developed from E1AF-transfected cells compared with vector-transfected cells. Tumorigenesis by E1AF has been investigated for breast tumors. E1AF is overexpressed in the vast majority of human breast cancers and in nearly all HER2/Neu–positive tumors (38). Using MMTV-Neu transgenic mice, Shepherd et al. (8) showed that expression of a dominant-negative E1AF transgene under the control of the MMTV promoter in mammary epithelial cells dramatically delayed the onset of mammary tumors and reduced the number and size of such tumors in individual mice. On the other hand, Xing et al. (39) reported that E1AF suppresses HER2 promoter activity in human tumor-derived cell lines, dependent on an E1AF binding site in this promoter, and inhibits tumorigenesis of the cells. However, several articles have shown that E1AF can activate E1AF-responsive promoters, including the human HER2/neu promoter in various cell types (3, 8, 40–42). Bojovic and Hassell (43) noted that the expression of these same genes is inhibited when E1AF protein is expressed at very high levels and suggested that transcriptional squelching accounts for these observations. Thus, both our results and observations in breast cancer indicate the tumorigenic activity of E1AF but this activity may depend on various conditions including cell type.

The development of mediastinal lymph node metastases from lung tumors of E1AF-transfected cells, but not from the lung tumor of vector-transfected cells, suggests that E1AF may enhance metastasis of NSCLC cells. These observations are consistent with previous reports showing that E1AF increases *in vivo* metastatic activities of fibrosarcoma cells (7) and breast cancer cells (44).

Highly phosphorylated MLC in the local and metastatic tumors developed from E1AF-transfected cells, suggesting an association between E1AF tumorigenic and metastatic activities and the increased activity of the Rho/ROCK pathway. Rho has been shown to have transforming activities (13, 14, 24) and may have some role in the observed tumorigenesis by E1AF. The association of Rho/ROCK signaling with metastasis is also consistent with recent reports showing that RhoC enhances metastasis of melanoma cells (28) and lung cancer cells (29) in association with migration and invasion.

In conclusion, these results suggest that E1AF induces activation of the Rho/ROCK pathway, which plays an important role for malignant phenotypes including motility and invasion as well as tumorigenesis and metastasis enhanced by E1AF in NSCLC cells. Inhibition of this pathway by molecules such as Y27632 may have therapeutic potential to control NSCLCs, most of which overexpress E1AF.

Acknowledgments

Received 1/7/2005; revised 8/3/2005; accepted 9/14/2005.

The costs of publication of this article were defrayed in part by the payment of page charges. This article must therefore be hereby marked *advertisement* in accordance with 18 U.S.C. Section 1734 solely to indicate this fact.

We thank Prof. Fumiaki Sasaki (Department of Pediatric Surgery, Hokkaido University Graduate School of Medicine) for suggestions and fruitful discussion.

References

1. Wasylyk B, Hahn SL, Giovane A. The Ets family of transcription factors. Eur J Biochem 1993;211:7–18.
2. Higashino F, Yoshida K, Noumi T, Seiki M, Fujinaga K. Ets-related protein E1A-F can activate three different matrix metalloproteinase gene promoters. Oncogene 1995;10:1461–3.
3. Xin JH, Cowie A, Lachance P, Hassell JA. Molecular cloning and characterization of PEA3, a new member of the Ets oncogene family that is differentially expressed in mouse embryonic cells. Genes Dev 1992;6:481–96.
4. Kaya M, Yoshida K, Higashino F, Mitaka T, Ishii S, Fujinaga K. A single ets-related transcription factor, E1AF, confers invasive phenotype on human cancer cells. Oncogene 1996;12:221–7.
5. Shindoh M, Higashino F, Kaya M, et al. Correlated expression of matrix metalloproteinases and ets family transcription factor E1A-F in invasive oral squamous-cell-carcinoma-derived cell lines. Am J Pathol 1996;148:693–700.
6. Hiroumi H, Dosaka-Akita H, Yoshida K, et al. Expression of E1AF/PEA3, an Ets-related transcription factor in human non-small-cell lung cancers: its relevance in cell motility and invasion. Int J Cancer 2001;93:786–91.
7. Habelhah H, Okada F, Kobayashi M, et al. Increased